The identification of genes involved in the degradation of polyphosphate in *Chlamydomonas reinhardtii*

A thesis presented in partial fulfilment of the requirements for the degree of

Master of Science

At Massey University, Palmerston North, New Zealand

Catarina Sofia Oliveira da Rocha

2021

Acknowledgements

The patience and support received throughout the research and writing of this dissertation was immense and not gone unnoticed.

To begin with, I would like to acknowledge the financial aid received by the Marsden fund, which allowed this research to proceed and produce meaningful results.

In addition, I would like to thank my supervisors, which without their support and help, the completion of the dissertation would not be possible. To Professor Benoit Guieysse, whose expertise was essential in the formulation of insightful questions, and for his valuable feedback and guidance. To Dr. Maxence Plouviez, your guidance and encouragement throughout the research was deeply appreciated.

Furthermore, I would like to acknowledge Mrs. Trish McLenachan for the support and advice throughout the genetic aspect of the research. Your experience and supervision were indispensable and profoundly appreciated.

Additionally, I would like to thank PhD-student Alex Cliff for all the support and helping-hand provided throughout the master's program.

And lastly, I would like to thank my parents, Eduardo Rocha and Felismina Silva, for their emotional and financial support throughout my under- and postgraduate studies. Your unconditional support was cherished and crucial. And to my partner, Shieneel Prakash for his support, love and helping hand when required.

Table of contents

Index of figures

Index of tables

Index of equations

Acronyms

%P – Hypothetical/Cellular P content

ADP – Adenosine diphosphate

ATP - Adenosine triphosphate

Cd - Cadmium

CDP – Cytidine diphosphate

CTP - Cytidine triphosphate

Ddp1 - Diadenosine and diphosphoinositol polyphosphate phosphohydrolase

DMSO - Dimethyl sulfoxide

EBPR - Enhanced biological phosphorus removal

Hg - Mercury

IPY1/IPY3/PPA - Soluble inorganic pyrophosphatase

MM low-P – Minimal media low-P

N - Nitrogen

Nudix – Nudix hydrolase enzyme

P - Phosphorus

PCR – Polymerase chain reaction

Pi – Inorganic phosphate

PO_4^{3-} - Phosphate

PolyP – Polyphosphate

PPi - Inorganic pyrophosphate

PPK - Polyphosphat kinase

PPN1 - Polyphosphatase

PPX – Exopolyphosphatase

qPCR – Quantitative polymerase chain reaction

S - Sulphur

TbNH2/TbNH4 – *T. brucei* Nudix Hydrolase 2 and 4

VTC - Vacuolar transporter chaperone complex

WSPs – Wastewater stabilization ponds

Abstract

Phosphate (P) is an essential nutrient which availability can limit the growth and survival of all organisms, including microalgae. Microalgae have been reported to absorb and accumulate P as polyphosphate (PolyP) intracellularly. This microalgal ability has interested engineers for years as it could prove valuable for P removal and recovery from wastewater. While a pathway for PolyP synthesis has been described in microalgae, little is known about the mechanisms involved during PolyP degradation in microalgae. In this study, a reproducible biochemical assay was designed to determine the kinetics of PolyP degradation in the model organism *Chlamydomonas reinhardtii*. For this purpose, *C. reinhardtii* wild-type 1690 was grown in minimal media low phosphorus (MM low-P) for 5 days prior to the addition of 10 mg L^{-1} P. Biological triplicates were analysed, and we measured the changes in cellular P content and granular-PolyP. After the analysis of the bioassays, we extracted RNA from the treatment groups.

Based on information reported in the literature regarding other organisms we selected *vtc1*, *vtc4*, *ipy1*, *ipy3*, *ppa* and *nudix hydrolase* as candidate genes encoding enzymes involved in PolyP degradation in *C. reinhardtii*. Quantitative PCR was used to measure the transcription of *ipy1*, *ipy3*, *ppa* and *vtc1* genes and these were shown to be regulated after the addition of P, but we were unable to quantify *vtc4* and *nudix* genes. To corroborate the transcriptomics data, we used insertional mutants knock down in IPY1, IPY3, PPA and Nudix hydrolase. The mutants were grown in ammonia acetate low phosphorus (low-P) media and we quantified the changes in cellular P content and granular-PolyP up to Day 13 (168-hours), after the addition of P. Based on our results, we selected Nudix hydrolase was the most likely candidate involved in the degradation of PolyP.

For the first time, we took a step to better understand PolyP consumption in microalgae. This knowledge is critical for a better understanding of the function and regulation of PolyP in algae.

Introduction

The excessive mining of 'fossil' phosphorus (P) is depleting the current finite and non-renewable P reservoirs at an alarming pace. As the global human population continues to increase (1.05% per year) (Roser et al., 2019), so will the demand for phosphorus to sustain agricultural outputs. However, plants are unable to absorb all the P supplied to them as fertilizer. The excess will infiltrate the soil and leach to the closest water bodies. As phosphorus is utilized by all living beings, the excess can be assimilated by microalgae resulting in rapid cell growth. This excessive growth, at the wrong time and place, ultimately leads to water eutrophication, a global issue (*e.g.* 30-40% of lakes are globally eutrophic) (Yang et al., 2008) which can be extremely nefarious for the environment. P-mediated eutrophication can also occur due to unproper P removal during wastewater treatment. Ironically as the organism mediating eutrophication, microalgae can also provide a solution to both 'cheap' P depletion and pollution. Indeed, microalgae already thrive in some wastewater treatment alternatives, such as stabilization ponds, but they are not removed from these systems, meaning P is merely transferred from an inorganic to an organic form, resulting in excessive cell growth. While microalgae harvesting still require specific development, inefficient P removal can be addressed by developing processes that enhance the microorganisms' natural ability to produce polyphosphate (PolyP) chains for cell growth and for prolonged survival in adverse conditions. However, while the pathway of PolyP synthesis has been described in the model alga *Chlamydomonas reinhardtii*, little is known about the pathway and enzymes involved in the degradation of PolyP in microalgae. Based on the knowledge of PolyP degradation in bacteria, yeast and *Trypanosoma*, the present research therefore aimed to identify the enzymes involved in PolyP degradation in *C. reinhardtii*. The results from this study aimed to improve our knowledge of PolyP consumption in microalgae. With further research, knowledge about PolyP function and regulation could ultimately help improve the current processes used to remove phosphate from microalgae-based wastewater treatment.

Section 1: Literature review

1.1. Phosphorus: a fast depleting resource

The global phosphorus (P) cycle has been significantly impacted by human activities over the past century. Many countries, including New Zealand, are dependent on P importation. For example, NZ$185 million worth of P rock was imported into New Zealand alone in 2012 (NZIER, 2012; NZIER 2014). Most of this P is mined from exhaustible sedimentary phosphorite deposits (Elser & Bennett, 2011; Cordell & White, 2011) and approximately 170 million tonnes of P rock are extracted per year (Mining Technology, 2016). Up to 90% of this phosphate is used for agricultural purposes, and the remaining P is used for the production of detergent and food (Adhya et al., 2015). The demand for P is increasing up to 2.3% per annum, largely due to an increasing demand for food production (Adhya et al., 2015). Consequently, all known good quality 'cheap' P reserves may cease to exist within the next 50 to 100 years (Scholz & Wellmer, 2013; Cordell et al., 2009; Steen, 1998), leaving only the lower quality and costly (uneconomical) P rocks available to extract (Smil, 2000; EcoSanRes, 2003). P reserves are unevenly distributed worldwide, with the majority present in Morocco (85%), followed by China (6%) and the United States of America (3%) (MacDonald et al., 2011). Current geopolitical tensions in area of Western Sahara are due to land area dispute and increase cost of P extraction, affecting the phosphate market and leading to a future of uncertainty (Kasprak, 2016).

In 2004, close to 25% of the 1 billion tonnes of phosphorus mined since the 1950s had ended up in water bodies or in landfills (Rosmarin, 2004). The leakage of phosphorus from agricultural land can lead to eutrophication of waterways (Sharpley et al., 2005). Eutrophication is defined as the excessive growth of primary producers (*i.e.* plant and algae) due to an increase supply of nutrients (generally nitrogen and phosphorus) that stimulates photosynthesis (Chislock et al., 2013). Eutrophication is usually unpredictable and hard to control (Rose & Dunn, 2013).

Due to the forecasted increasing cost of P extraction and geopolitical risks, an ideal solution would be to economically recover P from waste/wastewater and waterbodies and recycle this P back to

agricultural land. A potential method would be to harvest the microalgae that thrives in waste stabilisation ponds and are known to accumulate and store P to produce a biofertilizer (Ray et al., 2013).

1.2. P removal in wastewaters

Many small communities rely on waste stabilization ponds (WSPs) for wastewater treatment (Wichern et al., 2018), as they are economical to build and operate (Brown and Shilton, 2014). WSPs are suitable for removing pathogens (Curtis et al., 1992) and organic carbon (Powell et al., 2009) from domestic and industrial waste waters (Rose & Dunn, 2013). However, these systems are generally inefficient at P removal because dissolved P (in the form of phosphate) is not taken up enough by microorganisms and because these microorganisms are generally not removed from the treated water (meaning they ultimately decompose and most of the P initially assimilated into biomass is released as phosphate). Thus, only 15 to 50% of P is removed from influent wastewater (Garcia et al., 2000), and P-laden wastewater discharge into waterways can trigger eutrophication.

P is conventionally removed by chemical or biological technologies during large-scale 'centralized' wastewater treatment. The chemical methods used are effective but have significant issues. For example, the aluminium and iron salts used to precipitate phosphorus (Bolier et al., 1992) are unusable to plants, meaning that the sludge produced usually end up in landfills (Brown and Shilton, 2014). Enhanced biological phosphorus removal (EBPR) is a method where bacteria assimilate dissolved phosphorus in the wastewater and produce polyphosphate (PolyP) intracellularly. Yet, it is complicated to operate and costly for many small communities. (Brown and Shilton, 2014; Powell et al., 2009). Other P-removal methods have been tested in New Zealand, such as P adsorption by the melter slag that is produced when iron sand is transformed into molten iron (Bourke et al., 2005). Although the slag can remove up to 77% of dissolved P from WSP, altering the environment conditions, for instance pH, can reduce the efficacy of the slag by preventing P adsorption (Pratt et

al., 2007). On the other hand, microalgae are abundant in WSPs, and known to accumulate P into PolyP under certain conditions (Crimp et al., 2018; Powell et al., 2011). If it could be 'domesticated' (*e.g.* reliably triggered on demand) this ability could be used as a biological solution to aid the current P removal methods.

1.3. PolyP and its presence in microalgae

Microorganisms uptake dissolved phosphate for growth and, in specific circumstances, accumulate P under the form of PolyP, a linear polymer of three to hundreds of phosphate residues linked by high energy phosphoanhydride bonds (Kornberg, 1995; Achbergerová & Nahálka, 2011). PolyP has many functions in microorganisms, such as energy storage (Kornberg et al., 1956; Kornberg, 1995), phosphate storage (Harold, 1966; Moreno & DoCampo, 2013; Solovchenko et al., 2016), metal chelation (Archibald & Fridovich, 1982), alkaline buffering (Pick & Weiss, 1991), DNA transport (Castuma et al., 1995), or cell survival and stress regulation (Kornberg, 1995). PolyP also supports gene regulation (Tsutsumi et al., 2000), and might aid the formation of new genetic material (Jiménez et al., 2016). PolyP can be found in various location in cells according to it functions. For example, PolyP can be located in the cytoplasm, cell surface, periplasm or plasma membrane in bacteria (Kulaev, 1975; Wood & Clark, 1988). PolyP can be encountered virtually in any cell type in nature (Kornberg, 1995; Kulaev & Vagabov, 1983) since it can be used to support prolonged growth and survival of the organism in adverse conditions (Ray et al., 2013).

The ability to uptake and store P internally could provide a key competitive advantage to microalgae (Solovchenko et al., 2019). Microalgae can take up P at level higher than necessary to support the next life cycle, an ability known as luxury uptake (Rhee, 1973), and can then use PolyP during P deprivation conditions (Cembella et al., 1984a; Cembella et al., 1984b). This nutrient-driven process is common in natural ecosystems and, as mentioned above, in WSPs (Solovchenko et al., 2019; Crimp et al., 2018). Solovchenko and co-workers (2019) showed that the formation of PolyP occurs

rapidly in *Chlorella* strains after a high P influx, and later declines over time as the cells divide. Recently, there has been an interest in identifying the genes involved in the production of PolyP, however little is still known about the genes involved in PolyP degradation. Further analysis is therefore needed to determine the genes involved during PolyP degradation in microalgae. A future practical outcome of this research would be to understand how to regulate PolyP synthesis rather than PolyP degradation, and this understanding maybe lead to the development of a reliable and efficient P removal from microalgae-based wastewater treatment.

1.4. Genes and proteins involved in the production and consumption of PolyP

1.4.1. Bacteria

1.4.1.1. Polyphosphate kinase (PPK)

In the bacterium *Escherichia coli,* two known enzymes are involved in the synthesis of PolyP by transferring phosphate groups between PolyP and other phosphate-containing compounds. Polyphosphate kinase (PPK) catalyses the terminal phosphate of ATP to extend the PolyP chain (**Figure *1***; Kornberg, 1995; Downey, 2019). PPK enzymes are widely distributed in many organisms due to their role in the synthesis and degradation of PolyP chains (Kornberg et al., 1956). PPK enzymes play an important role in response to environmental change as for example, *ppk1 E. coli* mutants unable to produce PolyP have an increased sensitivity to hydrogen peroxide, high temperatures, and salt levels than their wild type (Rao & Kornberg, 1996). The main function of PPK enzymes is to shift energy and phosphate in both directions, either for storage or consumption (Achbergerová & Nahálka, 2011). Three PPK enzymes have been documented in bacteria: Polyphosphate kinase 1 (PPK1) catalyses the polymerization of the terminal phosphate of ATP to elongate the PolyP chain (**Figure *1***; Kornberg et al., 1956; Ishige et al., 2002). The enzyme PPK2 phosphorylates GDP to GTP using PolyP as a donor, through purine phosphorylation (**Figure *1***; Ishige et al., 2002). The enzyme can use GTP and ATP in the synthesis of PolyP chains, whilst PPK1 uses

exclusively ATP (Ishige et al., 2002). The third PPK enzyme discovered was PPK3, which uses inorganic PolyP as a donor to synthesise CDP to CTP, through pyrimidine phosphorylation (**Figure *1***; Nahalka & Patoprsty, 2009). In *E. coli,* the PPK1 enzyme is a histidine kinase that phosphorylates histidine residues during autophosphorylation. This event activates the enzyme to synthesise PolyP chains (Achbergerová & Nahálka, 2011).

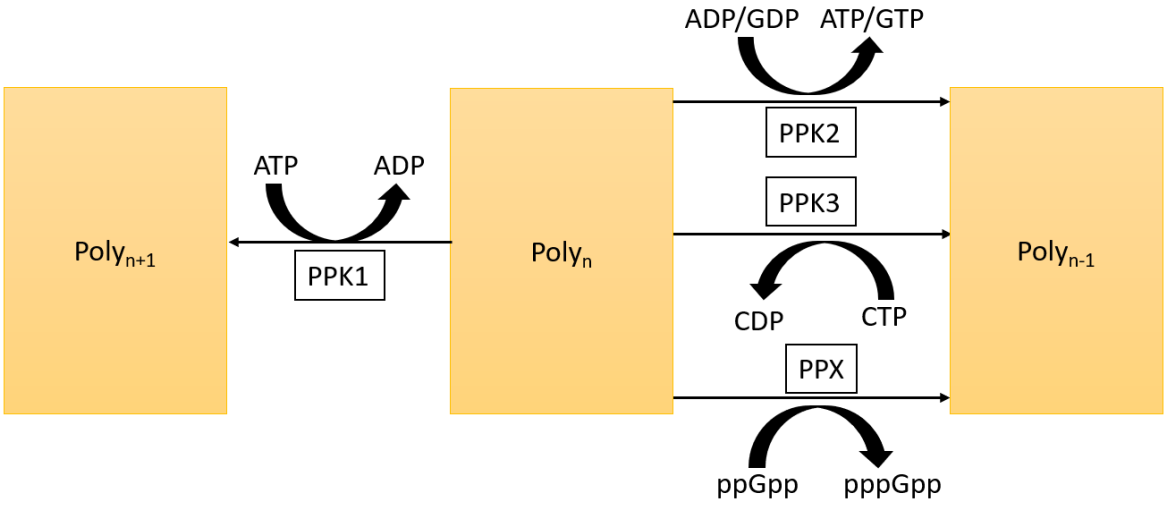

Figure 1: Graphical representation of PolyP production and degradation in bacteria by PPK enzymes (Based on Nahalka & Patoprsty, 2009; Wang et al., 2018). PolyP$_n$ represents a long PolyP chain which a P group was either added (PolyP$_{n+1}$) or removed (PolyP$_{n-1}$). ATP (Adenosine triphosphate), ADP (Adenosine diphosphate), GTP (Guanosine triphosphate), GDP (Guanosine diphosphate), CTP (Cytidine triphosphate), CDP (Cytidine diphosphate), Polyphosphate kinase (PPK1, PPK2, PPK3), Exopolyphosphatase (PPX).

1.4.1.2. Exopolyphosphatase (PPX)

Exopolyphosphatase (PPX) hydrolyses the phosphoanhydride bonds of a PolyP chain into free Pi, with a strong preference for long PolyP chains (Kornberg, 1995; Akiyama et al., 1992; Akiyama et al., 1993; Kornberg et al., 1999; Ahn & Kornberg, 1990). Downey (2019) analysed how the mutation of the *ppx* gene influenced the accumulation of PolyP inside *E. coli* cells. These authors concluded that both PolyP synthesis and consumption are regulated by PPK and PPX, respectively, and that PPX is

necessary for the degradation of PolyP (Gray & Jakob, 2015). The activity of the PPX enzyme fluctuates between synthesis and degradation of PolyP chains (Rao et al., 1998). The turnover of the PolyP chains is dependent on the cyclic hydrolytic breakdown caused by PPX and the PolyP accumulation caused by PPK (Rao et al., 1998; Kuroda & Kornberg, 1997). The mutation of the *ppx* gene in *E. coli* leads to a 100 to 1000-fold increase of PolyP (Kuroda & Kornberg, 1997). The genes encoding for the PPX and PPK enzymes are organized in a co-linear arrangement where the *ppx* gene is located downstream of the *ppk* gene. Hence, the translation and regulation of the *ppx* gene is dependent on the expression level of the *ppk* gene (Akiyama et al., 1992). In addition, PPK1 is part of the *E. coli* degradosome, which stimulates the degradation of mRNA by binding to the backbone rather than the 3' or 5' terminal phosphate of the RNA (Achbergerová & Nahálka, 2011). In comparison, PolyP inhibits the degradation of the mRNA by the degradosome (Blum et al., 1997). PPK has two main action mechanisms: it binds and degrades PolyP in the presence of ADP (Blum et al., 1997) and it participates in the cyclic hydrolytic breakdown of PolyP caused by PPX (Rao et al., 1998; Kuroda & Kornberg, 1997). These two processes influence the synthesis and degradation of the PolyP chain.

1.4.1.3. Inorganic pyrophosphatases

Soluble inorganic pyrophosphatase (ssPPase) is a ubiquitous enzyme. ssPPases can cleave a single inorganic pyrophosphate (PPi) to two inorganic phosphate (Pi) units (Gomez-Garcia et al., 2007) (**Figure 2**), hence it will have an effect on the P cycle. ssPPases are divided into two families: Family I, which can be found in all organisms (Cooperman et al., 1992) and Family II, which is restricted to certain bacteria and archaea (Young et al., 1998; Shintani et al., 1998). The ssPPase families are also sub-divided into two different types: ssPPases and proton-translocating PPases, both responsible for the hydrolysis of PPi and the replenishing of the Pi pool required for phosphorylation reactions (Gomez-Garcia et al., 2007). Since ssPPases are known to play an important role in the cellular P cycle of other eukaryotes such as yeast, it was hypothesized that microalgae might exploit enzymes that are similar in structure and function (homologues). Homologues of these proteins have already

been reported in other species, performing a similar role (Cooperman et al., 1992; Baykov et al., 1999; Lundin et al., 1991). In 2007, Gomez-Garcia et al. analysed the presence of two Mg^{2+}-dependent sPPases in *Chlamydomonas reinhardtii,* and they discovered two enzymes: PPA I and PPA II, located in the chloroplast and mitochondrion, respectively. In addition to PPAs, the inorganic pyrophosphatase family also includes members such as IPY1 and IPY3, was suggested to be involved in the energy/ATP metabolism pathway in *C. reinhardtii* (Michelet et al., 2008; Valledor et al., 2013).

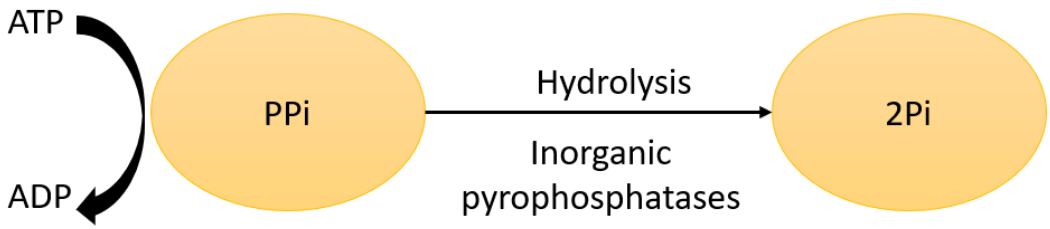

Figure 2: Graphical representation of PolyP degradation in bacteria by soluble inorganic pyrophosphatases enzymes (IPY and PPA). Inorganic pyrophosphate (PPi), Inorganic phosphate (Pi), ATP (Adenosine triphosphate), ADP (Adenosine diphosphate).

1.4.2. Yeast

1.4.2.1. Vacuolar transporter chaperone (VTC) complex

While *Saccharomyces cerevisiae* harbours no homologue of the genes encoding PPK enzyme present in bacteria, this yeast synthesizes PolyP through the vacuolar transporter chaperone (VTC) complex (Werner et al., 2007; Lonetti et al., 2011; Lichko et al., 2006). The synthesis and transport of PolyP is observed in vacuole-like organelle named acidocalcisomes (Hothorn et al., 2009; Gerasimaitė et al., 2014). The VTC subunits 1 to 4 form a hetero-trimeric protein complex where the yeast vacuolar membrane chaperon VTC4 acts as polyphosphate polymerase (DoCampo and Huang, 2016; Hothorn et al., 2009). In *S. cerevisiae*, Vtc4 was identified in the vacuolar membrane, and the polymerase reaction is accelerated by pyrophosphate (Hothorn et al., 2009). The VTC complex can exist in two forms according to its intracellular location: VTC4/VTC3/VTC1 complex found in the vacuole and

VTC4/VTC2/VTC1 complex found in the endoplasmic reticulum (Desfougères et al., 2016). The *S. cerevisiae* VTC proteins assemble into a complex (VTC1p-VTC4p) necessary for PolyP synthesis as well as several membrane-associated processes such as endocytosis, the organization of integral membrane ATPases, the transport of vesicles into the lumen of vacuoles leading to vacuolar-membrane fusion, and the transport of the vesicles between the endoplasmic reticulum and Golgi complex (Cohen et al., 1999; Ogawa et al., 2000; Müller et al., 2002, Müller et al., 2003; Uttenweiler et al., 2007). During its synthesis into the vacuole (also called acidocalcisome), PolyP is translocated into the vacuolar lumen, and can comprise up to 10% of the cell dry weight (Rao et al., 1998).

1.4.2.2. Exopolyphosphatase PPX and Polyphosphatase PPN1

Similar to bacteria, the genome of *Saccharomyces cerevisiae* also encodes the enzyme exopolyphosphatase PPX which hydrolyses the terminal orthophosphate from a PolyP chain (Kulakovskaya et al., 1997) (**Figure *3***). Another enzyme is the polyphosphatase PPN1, which has two functions: an endopolyphosphatase, degrading the PolyP chain into shorter fragments (Sethuraman et al., 2001; Shi & Kornberg, 2005), and an exopolyphosphatase, which fragments the orthophosphate of the end of the PolyP chain (Shi & Kornberg, 2005; Andreeva et al., 2006). The PPN1 polyphosphate activity is regulated depending on the growth phase, the stress conditions or even the location of the enzyme (Andreeva et al., 2015). The PPN1 enzyme is usually present in the vacuolar lumen (Lichko et al., 2006; Andreeva et al., 1998). Under certain growth conditions, the vacuolar lumen is acidic (Matile, 1978) and the optimal pH for the PPN1 is neutral (Andreeva et al., 1998). The alkalization of the vacuoles (caused by the excess of ammonium ions or heavy metal cations during stress) increases exopolyphosphatase activity, the breakdown of the PolyP chain and release of free orthophosphate (Andreeva et al., 2015). While magnesium (Mg^{2+}) enhances the enzymatic activity of the PolyP chain fragmentation, cobalt (Co^{2+}) stimulates the release of orthophosphate from the PolyP end chain (Andreeva et al., 2015). The regulation of the enzymes involved in the degradation of the PolyP granules varies throughout the cell cycle, possibly as a mechanism to conserve energy (Kulakovskaya et al., 2005). The studies by Kulakovskaya et al. (2005)

and Lichko et al. (2006) showed that the inactivation of the *ppn1* and *ppx1 S. cerevisiae* genes, respectively, caused a decreased activity of exopolyphosphatase in the cytosol leading to an increase of PolyP in the cytosol. Exopolyphosphatase activity may be regulated by posttranslational modifications (Andreeva et al., 2015).

1.4.2.3. Diadenosine and diphosphoinositol polyphosphate phosphohydrolase (Ddp1)

In 2011, Lonetti and co-workers analysed the possible existence of an additional endopolyphosphatase besides Ppn1 in *S. cerevisiae*, as previously suspected by Lichko and colleagues (2008). The authors discovered the presence of Ddp1 (Diadenosine and diphosphoinositol polyphosphate phosphohydrolase), an enzyme with a strong PolyP endopolyphosphohydrolase activity. Ddp1 is a homologue of the human diphosphoinositol polyphosphate phosphohydrolases (DIPPs). DIPPS hydrolyse inositol pyrophosphates, a phosphorylated molecule specific to eukaryotes (Bennett et al., 2006, Burton et al., 2009; Shears, 2009), and PolyP (Safrany et al., 1998). DIPPs also belong to the Nudix hydrolase family (Onnebo & Saiardi, 2009). In comparison, the Ppn1 enzyme is localized in the vacuole (Dove et al., 2002), whilst Ddp1 is localized in the cytosol, influencing the metabolism of PolyP (Huh et al., 2003).

1.4.3. Trypanosoma

1.4.3.1. Vacuolar transporter chaperone (VTC) complex

PolyP has an important role for the survival of *Trypanosoma* in harsh environments, especially during osmotic stress (Ruiz et al., 2001; DoCampo et al., 2011; Li et al., 2011). It was shown that PolyP is hydrolysed during hypoosmotic stress (Ruiz et al., 2001) and long PolyP-chains are produced during hyperosmotic stress in *Trypanosoma cruzei* (Ruiz et al., 2001; Li et al., 2011). Fang et al. (2007) discovered homologues of *S. cerevisiae vtc1* and *vtc4* genes in the genome of *Trypanosoma brucei* (*T. brucei*), a unicellular parasite. This lead to be further investigated by Lander and colleagues (2013) to determine the influence of said VTC enzymes in the production of PolyP in *T. brucei*. They

reported that TbVtc4 (*T. brucei* Vtc4) encodes a short chain PolyP kinase involved in the catalyses of PolyP in acidocalcisomes. The enzyme, however, is inhibited by PPi and only catalyses the production of short PolyP chains (Lander et al., 2013), nevertheless, they showed that PolyP was essential for cell viability and osmotic regulation (Ruiz et al., 2001; Lemercier et al., 2002; Fang et al., 2007; de Jesus et al., 2010; Li et al., 2011).

1.4.3.2. Nudix hydrolase family

T. brucei encodes five Nudix proteins, such as *T. brucei* Nudix Hydrolase 2 (TbNH2) and *T. brucei* Nudix Hydrolase 4 (TbNH4), which possess PolyP exopolyphosphatase and endopolyphosphatase activities, respectively (Cordeiro et al., 2019). TbNH2 is commonly found in the glycosomes while TbNH4 is found in the cytosol, as previously reported by Negreiros et al. (2018). Cordeiro and colleagues (2019) analysed the activity of TbNH2 and TbNH4 against $PolyP_{60}$ (short PolyP chain) and $PolyP_{700}$ (long PolyP chain). TbNH2 presented exopolyphosphatase activity by progressively removing the terminal P of the PolyP chains of, preferably, long PolyP chains (**Figure *3***). The protein also played a role on the conversion of ATP to ADP by releasing γ and β phosphates (Cordeiro et al., 2019) (**Figure *3***). On the other hand, TbNH4 presented two activities: endopolyphosphatase by attacking the internal phosphoanhydride bonds of PolyP molecules and exopolyphosphatase by removing Pi from PolyP chains of, preferably, shorter PolyP chains. The protein did not present any activity against ATP or ADP.

Both proteins have a role in the maintenance and regulation of PolyP in their respective locations (Cordeiro et al., 2019). Although the Nudix hydrolase family is present in eukaryotic species, including *C. reinhardtii*, little is known about the effect of the protein family on the degradation of PolyP in these species.

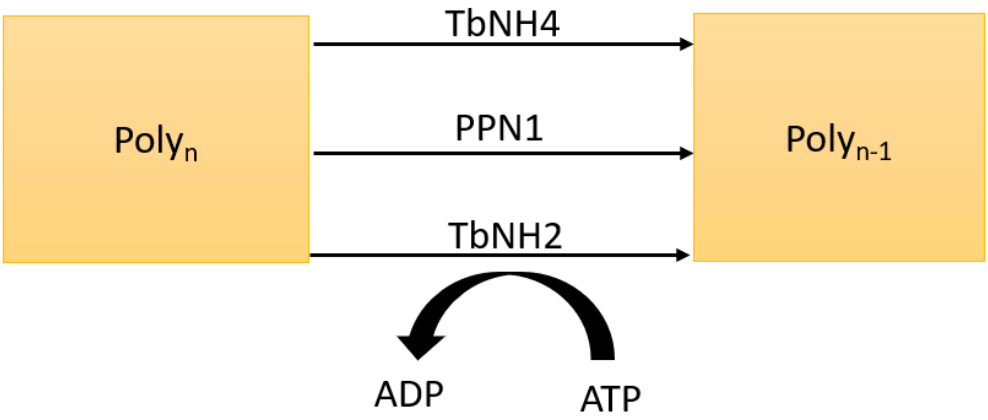

Figure 3: Graphical representation of PolyP degradation in yeast and Trypanosoma by PPN1, TbNH2 and TbNH4 enzymes). PolyPn represents a long PolyP chain which a P group was either added (PolyPn+1) or removed (PolyPn-1). ATP (Adenosine triphosphate), ADP (Adenosine diphosphate), TbNH2 and TbNH4 (T. brucei Nudix Hydrolase 2 and 4), PPN1 (polyphosphatase).

1.4.4. Microalgae

1.4.4.1. Vacuolar transporter chaperone (VTC) complex

PolyP accumulation also occurs in microalgae, with several species accumulating P up to 3.8% of their dry mass (Crimp et al., 2018). In the model species *C. reinhardtii,* PolyP granules are stored in acidocalcisomes (Ruiz et al., 2001; Achbergerová & Nahálka, 2011). This organelle accumulates cations (Ca^{2+}, Mg^{2+}, Zn^{2+}) essential for the maintenance of a vacuolar proton-pumping pyrophosphatase (V-H^+-PPase), an ATP synthase (V-H^+-ATPase), and the stabilization of PolyP (Ruiz et al., 2001). The *C. reinhardtii* genome encodes homologues of the subunits VTC1 and VTC4 of the *S. cerevisiae* VTC complex (DoCampo and Huang, 2016). This VTC complex is composed of four proteins: a small transmembrane protein (VTC1), and three proteins that contain transmembrane domains and a cytoplasmic segment (VTC2, VTC3 and VTC4) (Müller et al., 2003). VTC4 possesses a tunnel that generates PolyP from ATP, making it essential for the accumulation of PolyP inside the cell (Achbergerová & Nahálka, 2011). The lack of a functional VTC1 in *C. reinhardtii* mutants was shown to prevent the storage of PolyP inside the vacuoles (Aksoy et al., 2014). The elimination of the

VTC1 protein decreased the amount of visible acidocalcisomes, preventing the delivery of S- and N-responsive periplasmic proteins and altering the levels of PolyP within the acidocalcisomes by influencing the bio-energetic processes and membrane dynamics (Aksoy et al., 2014). Solovchenko and co-workers (2019) analysed the whole transcriptome of *Chlorella vulgaris* strains and *Parachlorella kessleri* CCALA 251 and selected potential genes involved during PolyP synthesis by microalgae cells. These authors found transcripts encoding a VTC-like protein, a H^+/Pi symporter, a Na^+/Pi symporter and a purple acid phosphatase. The transcript of VTC-like proteins decreased after the cells were supplied P and increased dramatically during the stationary phase, becoming 47-fold higher in P-replete than P-starved cells. Thus, Solovchenko and co-workers (2019) suggested that VTC-like proteins are involved in the biosynthesis of PolyP. Using *C. reinhardtii* mutant strains, Plouviez et al. (2021) showed that while *vtc1* and *vtc4* mutants never synthesize PolyP, vtc1 and vtc4 rescued phenotype were able to synthesize PolyP. This evidence confirmed the role of the VTC complex during PolyP synthesis in *C. reinhardtii*.

1.4.5. Genes potentially involved in PolyP degradation in algae

As stated above, in bacteria, inorganic pyrophosphatases (*i.e.* PPA (I), IPY1 and IPY3) are involved in the hydrolysis of P complexes, such as PPi, and the maintenance of Pi pools for cell function, while the Nudix hydrolase family plays an essential role in *T. brucei* by degrading PolyP chains. Other genes, such as *ppx*, *ppk* and *ppn1*, although also involved in the production and degradation of PolyP, were not found in homologue searches within the *C. reinhardtii* genome (process detailed in section 2.4.7.). Consequently, it is pertinent to analyse the *C. reinhardtii* candidate genes *ppa (I)*, *nudix*, *ipy1* and *ipy3* due to their potential involvement in the degradation of PolyP.

1.5. Parameters potentially influencing PolyP metabolism in microalgae

1.5.1. Cadmium

Nishikawa and co-workers (2003) analysed the effect of cadmium (Cd) on the microalga *Chlamydomonas acidophila*. The strain used was adapted to acidic environments and heavy-metal toxicity. The authors measured the effects of 10 or 20 µM Cd for 1, 2 and 3 days on a modified Sager-Granick Medium. These authors concluded that Cd causes a decrease in the concentration of PolyP, correlated with the increase of Cd inside the vacuoles, 3 days after Cd supply. Cells treated with 20 µM Cd also presented dramatic vacuole morphometric changes. Re-inoculation of Cd-treated cells on Cd-free media could not rescue P levels back to original level.

1.5.2. Sulphur

In 2014, Aksoy and co-workers characterized a *Chlamydomonas* mutant *ars76* (gene deleted or disrupted) unable to properly acclimate to S deprivation. The authors maintained the cells in TAP-S (tris-acetate-phosphate without sulphur) agar medium and sprayed the colonies with a 10 mM solution of 5-bromo-4-chloro-3-indolyl sulphate, one week prior to the ARS test. The mutant was unable to accumulate extracellular arylsulfatases (ARSs), which prevented the cells from scavenging extracellular SO_4^{2-} (Aksoy et al., 2014). In addition, the mutant poorly adapted to the deprivation of other nutrients, reducing the survival of cells in the absence of both P and nitrogen (N) due to poor acclimatization (Aksoy et al., 2014). The mutant phenotype was rescued after the complementation of one deleted gene, *vtc1*. The *ars76* mutant exhibited normal phosphatase activity under P starvation; however, the mutant was unable to acclimate to S deprivation, showing that the VTC1 protein is necessary for S and P acclimatization (Aksoy et al., 2014).

1.5.3. Mercury

Mercury (Hg) is another element that could affect PolyP degradation. Microalgae can accumulate toxic metals such as Cd^{2+}, Cu^{2+}, and Zn^{2+} in their cell wall (Macfie et al., 1994), and an increased number of electron-dense deposits inside vacuoles (Nishikawa et al., 2003; Aguilera and Amils,

2005). Samadani & Dewez (2018) compared how a wild-type (CC-125) and a cell-wall deficient (CC-503) strain of *C. reinhardtii* were affected by different levels of Hg. The authors exposed the *C. reinhardtii* strains to 0, 1, 3, 5 and 7 µM concentrations of $HgCl_2$ in a final volume of 25 mL of HSM (high salt medium) for 72h when cells reached a concentration of $5x10^5$ cells mL^{-1}. Hg had an inhibitory effect on cell density, and this effect was correlated with the concentration of Hg supplied and the time of exposure, ultimately causing cellular necrosis in both strains (Samadani & Dewez, 2018).

1.5.4. Ammonium

Ruiz-Martinez et al. (2014) analysed the effect of P-starvation on the rate of ammonium uptake in wastewater treatment plants and found that supplementing the liquid medium with P was associated with an increase in the amount of PolyP in the biomass as well as an increase in the N removal rate. After comparing the different reactors, they concluded N uptake was associated with the cellular P content of the cell. There might be a relationship between N and P removal due to their function in cells (Güsewell, 2004): hence, both nutrients could stimulate cell growth when abundant and, when their levels become limiting again, the microorganism would conserve the remaining nutrient reservoirs.

Table 1: Chemical influencing PolyP synthesis and consumption in microalgae

Species	Trigger	Comments/ Reference
Chlamydomonas reinhardtii	Cadmium (Cd^{2+})	Cd^{2+} absorption was correlated with PolyP degradation. Cd^{2+} is found in vacuoles with Pi residues (Nishikawa et al., 2003)
Chlamydomonas species	Sulphur	S is necessary for cell growth; its deficiency leads to reduced cell survival. Mutants defective in ARS do not properly acclimate to S and P deprivation (Aksoy et al., 2014)
Chlamydomonas reinhardtii	Mercury	The presence of at least 5 and 7 µM of Hg prevents the cells from accumulating PolyP leading to a decline in cell density and necrosis (Van Veen et al., 1994a, 1994b; Keasling, 1997; Samadani & Dewez, 2018)
Microalgal culture	Ammonium	Stimulates P uptake leading to fast cells growth, hence fast depletion of PolyP storage (Ruiz-Martinez et al., 2014)

1.5.5. PolyP consumption

Nishikawa and co-workers (2006) showed that *C. reinhardtii* C-9 and *C. acidophila* KT-1 could produce PolyP. *C. reinhardtii* C-9 produced 2.5 times more PolyP granules than *C. acidophila* KT-1; however, the granules were degraded faster in the C-9 strain. After nearly 6 days post P-supply, PolyP granules were barely visible in both strains (Nishikawa et al., 2006). Although the literature available about potential triggers for PolyP degradation is limiting, Powell et al. (2009) verified that light intensity had a positive effect on cell growth leading to decreasing internal P stores in microalgae. In prokaryotes, cations such as Mg^{2+} and Co^{2+} act as cofactors for PolyP degrading enzymes (Andreeva et al., 2015), and it is unknown if these cations have a similar role in eukaryotic species.

As stated in Sections 1.5.1. to 1.5.4., cadmium and mercury have a direct influence on the accumulation or degradation of PolyP, respectively. On the other hand, ammonium and sulphur have an indirect influence, as the nutrients stimulate P absorption and cell growth. Consequently, studying the effects of mercury and cadmium will provide information regarding PolyP degradation without needing to consider simultaneous effects on growth.

1.6. Literature review conclusions and future objectives

The extensive use of P fertilizers for food production is causing the rapid depletion of 'cheap' fossil P reserves. There is therefore a need for recovering and recycling this valuable resource. One solution could be to harvest the P-absorbing microalgae commonly found in natural systems and WSPs and use this biomass as a biofertilizer. However, to do this we must first understand the molecular basis for PolyP synthesis and consumption in microalgae so that this ability can be reliably triggered 'on demand'. Looking more broadly, unravelling how algae sense, uptake, store, and use P is critical to better understand the mechanisms behind eutrophication and, consequently, to better predict and

manage P pollution. This knowledge has also the potential to provide new engineering fundamentals in algal biotechnology.

Some of the key genes involved in the synthesis of PolyP in *C. reinhardtii* have been documented but the genes involved in PolyP consumption, and the triggers that influence this consumption, remain largely unknown in microalgae. Based on the current knowledge of *C. reinhardtii* and other organisms, we have identified *ppa*, *nudix*, *ipy1* and *ipy3* as potential genes involved in PolyP consumption. In addition, we also identified potential triggers of PolyP consumption, such as mercury, sulphur, ammonium and cadmium.

1.6.1. Research objectives and aim

Previous research has shown that microalgae absorb dissolved P and readily convert it into PolyP. However, little is known about its degradation in microalgae. Using bioassays and quantitative PCR (qPCR), this research will seek to characterize the kinetics of PolyP consumption in the model microalgae species *C. reinhardtii* (selected due to its well documented genome and prior research), will be grown in minimal media low-P (MM low-P) for 5 days, and control (no P supplied) and treatment (single 10 mg L^{-1} P dose supplied) groups will be analysed. We will thus look for conditions that trigger a rapid consumption of PolyP inside the cells and their effect on P kinetics. Furthermore, based on the bioassays results and with the aid of qPCR, we then aim to identify the genes involved in the consumption of PolyP in this model species.

1.6.2. Research plan

1. Select a suitable methodology based on the literature;
2. Develop reproducible protocols (with positive & negative controls), to characterize the kinetics of PolyP consumption in *C. reinhardtii;*
3. Identify candidate genes (from the literature) and verify their presence in *C. reinhardtii*;

4. Conduct qPCR on positive vs negative control, to confirm/quantify the expression of genes involved during PolyP consumption;

5. If qPCR is unsuccessful, we will consider RNAseq to identify the genes involved.

6. Evaluate the influence of triggers (from literature) on PolyP consumption kinetics and candidate gene expression in *C. reinhardtii*;

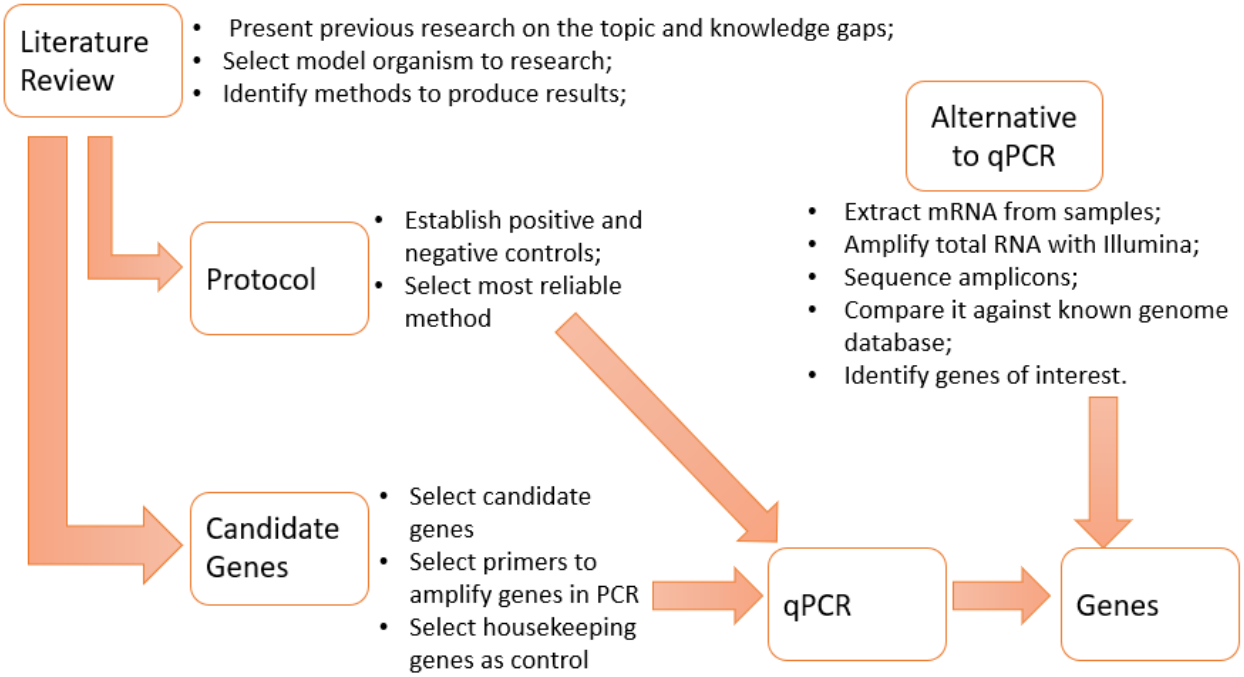

Figure 4: Prospect plan.

Section 2: Materials and methods

2.1. Culture maintenance and preparation of inoculum

C. reinhardtii 1690 was maintained on solid agar minimal media (15 g Agar·L^{-1}, agar-agar from Merck). The chemical composition of the minimal media can be found in the appendix (**Table *7***). Axenic cultures were kept at room temperature under ambient light for 4 weeks.

C. reinhardtii 1690 strain was also grown axenically on liquid minimal media containing 1 mg-P/L (low-P MM; Appendix **Table *7***). For this purpose, 15 -40 mL of the cultures were inoculated on 100 mL low-P MM (200-250 mL) in Erlenmeyer E-flasks. E-flasks were kept in an incubator at 25°C ± 2°C under continuous illumination (21 µmol·$m^{-2}s^{-1}$ PAR) and orbital agitation at 165 rpm. CO_2 levels were maintained at 2.0± 0.1% (v/v). Glassware and media were prepared and autoclaved on a weekly basis.

The IPY1, IPY3, PPA and Nudix mutant strains required a modified media to allow cell growth (**Table 8**). During the experiments, around 10 mL of culture was inoculated in 100 mL of Ammonia acetate low-P media in E-flasks. The E-flasks were maintained as detailed above. The media and glassware were autoclaved prior to inoculation.

2.2. Bioassays

2.2.1. C. reinhardtii 1690 wild type strain

Each experiment was conducted over a two-week period. On Day 1, 20 - 40 mL of C. reinhardtii 1690 culture was inoculated into 100 mL low-P MM in E-flasks and incubated under the conditions described in Section 2.1. The cultures were kept in those conditions for 5 days to create P deplete conditions. As detailed in The abilities of IPY1, IPY3, PPA, Nudix and wild-type 4533 strains to produce and consume PolyP was assessed using the protocol described in **Table 2**. On one occasion,

one E-flask (treatment group) was kept for 168-hours post P-shot for further analysis: and a 10 mL sample was withdrawn for visual analysis of PolyP degradation (software analysis).

Table 2, 25 mL of sample was withdrawn on Day 6 prior to the addition of 10 mg L^{-1} P of P solution (P-shot). On days 7, 8 and 9, 10 mL of culture was removed to record optical density (OD), cell count, dissolved phosphate concentration (DP), and the presence of granules. On day 6 and 10, 25 mL of culture was withdrawn to measure OD, CC, DP, total phosphorus (TP), dry weight (DW), and staining. The three treatment groups analysed were 1) Single-supply (single 10 mg L^{-1} P supply after 0-hours sampling); 2) Dark (single 10 mg L^{-1} P supply after 0-hours sampling and covered with aluminium) and 3) Fed-batch (10 mg L^{-1} P supply after 0-hours sampling and low 2 mg L^{-1} P supply every 24-hours after).

2.2.2. IPY1, IPY3, PPA, Nudix, and wild-type 4533 strain

The abilities of IPY1, IPY3, PPA, Nudix and wild-type 4533 strains to produce and consume PolyP was assessed using the protocol described in **Table 2**. On one occasion, one E-flask (treatment group) was kept for 168-hours post P-shot for further analysis: and a 10 mL sample was withdrawn for visual analysis of PolyP degradation (software analysis).

Table 2: Detailed timeline of experiment for the analysis of *C. reinhardtii* strains. *C. reinhardtii* 1690 strain was analysed till day 10 (96-hours post P-shot). The IPY1, IPY3, PPA, Nudix and wild-type 4533 strains were also analysed till day 13 (168-hours).

Day 1	**Day 2**	**Day 3**	**Day 4**	**Day 5**	**Day 6**	**Day 7**
1st day of starvation					P-shot (OD, CC, DP, TP, DW, and staining)	24-hours post P-shot (OD, CC, DP, and staining)
Day 8	**Day 9**	**Day 10**	**Day 11**	**Day 12**	**Day 13**	**Day 14**
48-hours post P-shot (OD, CC, DP, and staining)	72-hours post P-shot (OD, CC, DP, and staining)	96-hours post P-shot (OD, CC, DP, TP, DW, and staining)			168-hours post P-shot* (staining)	

2.2.3. Starved C. reinhardtii samples

C. reinhardtii 1690 strain was grown in the same conditions as stated on Section 2.1., however samples were removed daily (every 24-hours). RNA was extracted from the samples in order to perform qPCR and to quantify the changes in genes expression of the selected genes during P-deplete conditions (no P supplied) (**Table 3**).

Table 3: Summary of the experiments performed.

Species	Media used	Starvation period	Group	Initial P	Additional P	Measurements
C. reinhardtii 1690	Minimal media low phosphate	5 days	Single-shot	10 mg/L	N/A	OD, DP, TP, Staining, CC, DW
			Dark	10 mg/L	N/A	OD, DP, TP, Staining, CC, DW
			Fed-batch	10 mg/L	2mg/L every 24h	OD, DP, TP, Staining, CC, DW
C. reinhardtii IPY1, IPY3, PPA, Nudix mutants and WT 4533	Ammonium acetate low phosphate media	5 days	Control	N/A	N/A	OD, DP, TP, Staining, CC, DW
			Treatment	10 mg/L	N/A	OD, DP, TP, Staining, CC, DW
C. reinhardtii 1690	Minimal media low phosphate	12 days	Control	N/A	N/A	OD, DP, TP, Staining, CC, DW

2.3. Analysis

2.3.1. Cell growth

Cell growth was either determined by optical density (OD), cell count, or dry weight:

- OD was determined by measuring absorbance at 683 nm using a spectrophotometer (UV-1800, Shimadzu; Serodio et al., 2009). This measurement provides a rapid proxy for cell growth.
- For cell counting, a culture sample was firstly diluted using Trypan Blue solution (0.4%) in order to distinguish dead from viable cells. After dilution, 10 µL of sample was placed in a haemocytometer covered with a cover slip (modified methods of Song et al., 2018). Cells

were visualized and photographed under 10x magnification (Olympus BX53). The image of the cells was manually counted.

- For dry weight (DW) quantification, glass fibre filters previously dried at 105°C for 24 hours, were pre-weighed on the day of the experiment. A known volume (2.5-5 mL) of culture sample was then loaded onto the filter and excess liquid was removed by vacuum filtering. The same volume of water was added to remove excess salts. The filters were finally dried for at least 2 hours at 105°C before final weight was quantified. The dry weight (DW) was calculated following **Equation *1*** (Sells et al., 2018):

$$DW = \frac{(Wf - Wi)}{V}$$

Equation 1: Dry weight equation (DW). DW stands for the cell weight concentration ($g \cdot L\text{-}1$), Wf stands for final weight (g), Wi stands for initial weight (g) and V stands for volume of culture used for the filtration (L).

2.3.2. PolyP Granule

300 µL of microalgal culture was fixed on a microscopic slide by heat-fixing the sample at 105°C for 5 min. These samples were then stained with lead-sulphide as described by Bolier et al. (1992). For this purpose, the slides were treated with lead nitrate solution (2.5 g $Pb(NO_3)_2$ in 100 mL HNO_3, 5%) for 5 minutes, followed by ammonium sulphide solution treatment (NH_4S, 20% in H_2O, from Sigma-Aldrich) for 12 seconds. Distilled water was then used to rinse between each step. The slides were observed and photographed with a light microscope (oil immersion and 100x magnification) to observe the presence of PolyP granules. The PolyP granules were analysed manually and through a software analysis program (ImageJ). The use of lead-sulphide is a quick, reasonably inexpensive method to detect cellular granular-PolyP in microalgal cells. The method relies on the substitution of counter-ions of the phosphate polymers by lead-ions (Bolier et al., 1992).

2.3.3. Phosphate analysis

Dissolved phosphate (PO_4^{3-}) concentration was quantified using an ion chromatograph (Thermo Scientific, Dionex ICS-2100, Dionex IonPac AS11-HC column and AG11-HC guard column), after filtering culture samples using a 0.45 µm Minisart filter by Sartorius (Sells et al., 2018).

Assuming all the dissolved P removed from cultures was assimilated into biomass, the phosphorus content of the algal biomass (%P) was calculated as:

$$\%P = \frac{(TP - DP)}{DW} \times 100\%$$

Equation 2: Equation for indirect measurement of cellular phosphate. %P is the percentage phosphorus per unit dry weight (g-P·g-DW-1), TP is the total phosphorus (g-P·L-1), DP is the dissolved phosphorus in the solution (g-P·L-1), and DW is the dry cell weight.

Total phosphate concentration was quantified using TNT 843 kit [(HACH, sulfuric acid/persulfate digestion and the ascorbic acid method (equivalent to EPA 365.1)].

2.3.4. Statistical analysis

A student T-test ($\alpha = 0.05$) was used to determine the statistical significance of the data collected. In addition, we also checked for outliers. To verify the presence of outliers, we either presented the data as a box-plot graph or, calculated the upper and lower quartiles and verified if any data point fell outside of the change.

2.4. Genetics

2.4.1. Introduction to qPCR

Quantitative real-time polymerase chain reaction (qPCR) is an important tool to analyse gene expression (Kuang, et al., 2018). PCR was first developed in 1985 by Kary Mullis (Mullis & Faloona, 1987), followed by qPCR (Higuchi et al., 1993) which can be used to study a wide range of samples from many sources, such as blood, and many cell types (Kuang, et al., 2018). Several steps need to be followed from acquiring the sample to the analysis of the results including: (1) acquisition and proper handling of the experimental samples; (2) extraction of the total RNA from the samples; (3) analysis of the concentration and quality of the RNA sample; (4) reverse transcription of mRNA into cDNA; (5) optimization of the conditions for the qPCR assay; (6) accurate measurements of the expression of the genes of interest under optimized conditions; and, (7) normalization of the results (Kuang, et al., 2018).

2.4.2. Selection of RNA extraction methods

Depending on the cost of the extraction kit and RNA concentration, certain methods will provide more benefits than others. Careful evaluation of the methods available and accuracy will allow the selection of the most appropriate method used in this study.

Tesena et al. (2017) compared the RNA quality/quantity of column-based extractions (ZR RNA MiniPrep) against phenol-based extractions (TRIzol and GENEzol reagents) using animal tissue as the sample. In addition, comparisons between qPCR master mixes were performed, which included qPCRBIO SyGreen Mix, KAPA SYBR FAST qPCR Master Mix, QuantiNova SYBR Green PCR Kit and PerfeCTa SYBR Green SuperMix. These authors concluded that ZR RNA MiniPrep performed better than TRIzol and GENEzol reagents, with the lowest protein contamination and best RNA quality. After selecting the 'ideal' RNA extraction kit, the authors analysed which PCR mix performed better at amplifying the genes of interest. Tesena et al. (2017) thus determined that KAPA mix had a higher sensitivity, by amplifying RNA at a lower concentration (10 ng). The different results were due to the

kits themselves (Chomczynski & Sacchi, 1987), as both TRIzol and GENEzol reagents are phenol-based solutions, presented a similar yield of RNA extracted however, GENEzol had a higher RNA purity (Tesena et al., 2017). While, the column-based extraction was selected as the best option for RNA extraction, it has a superior cost when compared to the phenol method (Tesena et al., 2017). Similar conclusions were observed about the PCR mixes, since their different in gene detection efficiency could be due to the commercial DNA polymerase kit (Arezi et al., 2003; Purzycka et al., 2006). Column-based RNA extractions, including ZR RNA MiniPrep, produced better RNA quality and KAPA mix had a higher sensitivity. We concluded that the column-based RNA extraction method could provide benefits to our study.

2.4.3. RNA extraction (Trizol™ Plus RNA Purification Kit)

Ten (10) mL of inoculum sample was withdrawn at 0-, 24-, 48-, 72- and 96-hours and transferred into a 15 mL falcon tube. The samples were centrifuged at maximum speed (4,000 g) for 3 to 5 minutes, depending on cell concentration. The supernatant was removed, and the cell pellets were stored at -80°C till RNA was extracted. For RNA extraction, the samples were kept on ice during defrosting and RNA was extracted using TRIzol™ Plus RNA Purification Kit according to the manufacturer protocol (Thermo Fisher, USA). Protocol was detailed in the appendix.

2.4.4. Contamination removal

2.4.4.1. DNAse treatment

The DNAse treatment is a necessary step to concentrate the RNA samples (smaller volume) and remove contaminants such as protein and DNA. For this purpose, 50 µL of the 100 µL of RNA extracted was transferred to a clean 1.5 mL microtube and the protocol followed was detailed in the appendix.

2.4.5. RNA concentration

RNA concentration and quality were quantified using Qubit and NanoDrop (see below). The identification of contaminants can determine potential PCR inhibitors.

2.4.5.1. Qubit (ThermoFisher)

A Qubit fluorometer was used to measure the RNA concentration of the samples before and after the DNAse treatment. In this study, we analysed 3 µL of RNA sample to measure the concentration of the RNA extracted. Protocol followed was detailed in the appendix as per the manufacture instructions.

2.4.5.2. NanoDrop (ThermoFisher)

NanoDrop was used to measure the RNA concentration and quality of the samples before and after the DNAse treatment. Clean Nanodrop with 2 µL of water to calibrate machine. Transfer 2 µL of sample to measure RNA concentration, and the ratio of 280/260 and 260/230 for possible protein or a reagent, such as phenol, residual contamination.

2.4.6. Reverse transcriptase

In order to measure the gene expression of the sample through qPCR and/or amplify the RNA sample through PCR, the RNA needs to be converted into cDNA.

2.4.6.1. qScript™ XLT cDNA SuperMix

Samples were prepared under a sterile fumehood and kept on ice during the experiment. Protocol followed was detailed in the appendix as per the manufacturer's instructions.

2.4.7. PCR amplification

During the first analysis of the efficiency of the primer sets, PCR was used to determine if the primers were annealing in the correct area by producing the right-sized amplicon.

2.4.7.1. EmeraldAmp GT PCR Master Mix (2x)

Samples were prepared under a sterile fumehood and kept on ice during the experiment. Protocol followed was detailed in the appendix as per the manufacture instructions.

2.4.8. qPCR amplification in a LightCycler 480

cDNA samples were analysed through qPCR to quantify the gene expression of the samples of interest. Different primer sets (genes) were tested in different 96-well plates due to the different annealing temperatures required.

Samples were prepared under a sterile fumehood and kept on ice during the experiment. Protocol followed was detailed in the appendix as per the manufacture instructions.

2.4.8.1. Analysis of LightCycler 480 results

Data extracted from the LightCycler was analysed as detailed in the appendix.

2.4.9. BLAST analysis

To verify if the certain genes, such as *ppx*, *ppk* and *ppn1,* commonly found in bacteria and yeast could also be present in microalgae, we used BLAST[1] to search for homologues. Firstly, we found the sequence encoding the selected genes in bacteria and yeast (UniProt) and searched it on BLAST using blastx (nucleotides to protein) and nucleotide blast (nucleotide to nucleotide) against *C. reinhardtii* genome. Unfortunately, the sequence similarity was too low to be considered homologous. Hence, we analysed *ipy1*, *ipy3*, *ppa* and *nudix* genes since they were already found in *C. reinhardtii*.

[1] BLAST (https://www.ncbi.nlm.nih.gov/books/NBK153387/)

Section 3: Results & Discussion

3.1. Bioassays

Prior to the collection of the presented data, we developed a reproducible protocol. The protocol was previously detailed by Sells and colleagues (2018). However, some steps were slightly altered to fit the new circumstances. The main change was the time frame, since the protocol was previously used to analyse PolyP synthesis rather than degradation, as it was in our case. The second change was how TP was measured. Sells and colleagues (2018) used sulphuric acid-nitric acid digestion with ascorbic acid colourimetry. In our case, we used TNT 843 kit, similar process, but easier, quicker and reliable in the measurement the granular and non-granular PolyP.

After adjusting the protocol, we quantified the changes in the hypothetical cellular P content (henceforth called P cellular content for simplicity, %P) and visual quantification of granular-PolyP in *C. reinhardtii* cells (see methods and materials section). For this purpose, we grew *C. reinhardtii* 1690 strain in low-P MM for 5 days prior to adding either a 'single supply' of 10 mg L^{-1} P (single-supply and dark group) or a supply of 10 mg L^{-1} P followed by additional daily supplies at 2 mg-P·L^{-1} (fed-batch group) for the remaining duration of the experiment. In addition, the dark group flasks were wrapped in aluminium foil after the initial single P-shot.

3.1.1. Analysis of hypothetical cellular P content (%P)

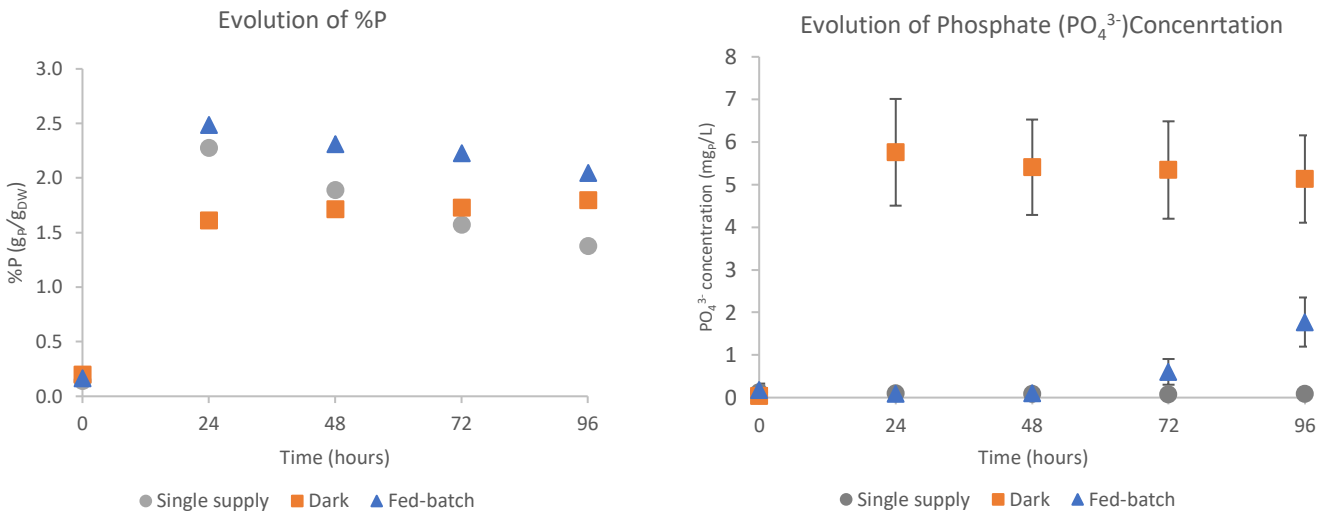

Figure 5: Evolution of hypothetical cellular P content (%P; Left) and extracellular PO_4^{3-} concentration (Right) of the single-supply group (two data points at 0-hours were identified as outliers and removed), dark group and (one data point at 72- and 96-hours were identified as outliers and removed). Number of replicates varied between 6 and 15.

At 0h, the cellular P content was not statistically different among the 3 treatments (p-value > 0.05, t-test) and averaged 0.16 ± 0.02 %P. Due to the conditions of the culture and the absence of granules in the cells (Appendix, **Figure *17***), this initial average P cellular content represents the P incorporated into structural cellular components (*e.g.* membranes and nucleic acids).

Dissolved PO_4^{3-} concentration decreased to nearly undetectable levels, 24-hours after P addition, in the single-supply group (**Figure *5***, right), whilst the P cellular content increased from 0.14 ± 0.04 % initially to 2.27 ± 0.42 % 24-hours after P addition. Over the next 72-hours, P cellular content gradually decreased to reach 1.38 ± 0.22 % (**Figure *5***, left). PO_4^{3-} was not completely assimilated and remained above 5 mg/L during the experiment.

Cells initially kept in darkness assimilated up to two thirds of the 10 mg L^{-1} P initially supplied (**Figure *5***, right). The dark culture continued to slowly absorb P throughout the experiment, leading to an increase of cellular P content up to 1.80 ± 0.40% 96 hr after the initial P supply (**Figure *5***, left).

In the fed-batch group, cellular P content increased to 2.49 ± 0.39% at 24-hours and decreased to 2.05 ± 0.25% over the next 72-hours (**Figure *5***, left). PO_4^{3-} concentration decreased to nearly zero in the first 24-hours (**Figure *5***, right). However, likely due to the daily P supply, PO_4^{3-} concentration started to increase at 72-hours.

As evidenced by the data described, *C. reinhardtii* 1690 quickly assimilated PO_4^{3-} (<24-hours) in the single-supply and fed-batch groups. This uptake was associated with an increase in hypothetical cellular P content within the first 24- to 48-hours. Cells kept in darkness behaved slightly differently as the P supplied was only partially up taken. Cultures of *Chlamydomonas* (Goodenough et al, 2019) and *Chlorella* (Aitchison & Butt, 1973) grown under P-replete and light limited conditions do not accumulate extensive P reservoirs in the absence of stressors (Slocombe et al., 2020). Lack of light has a repressive effect on the degradation of P storage (Powell et al., 2009). As PolyP might be essential for energy regulation (production of ATP) (Kornberg et al., 1956; Kornberg, 1995), the lack of light could have partially repressed the need for internal energy in the photosynthetic cells.

3.1.2. Cellular growth

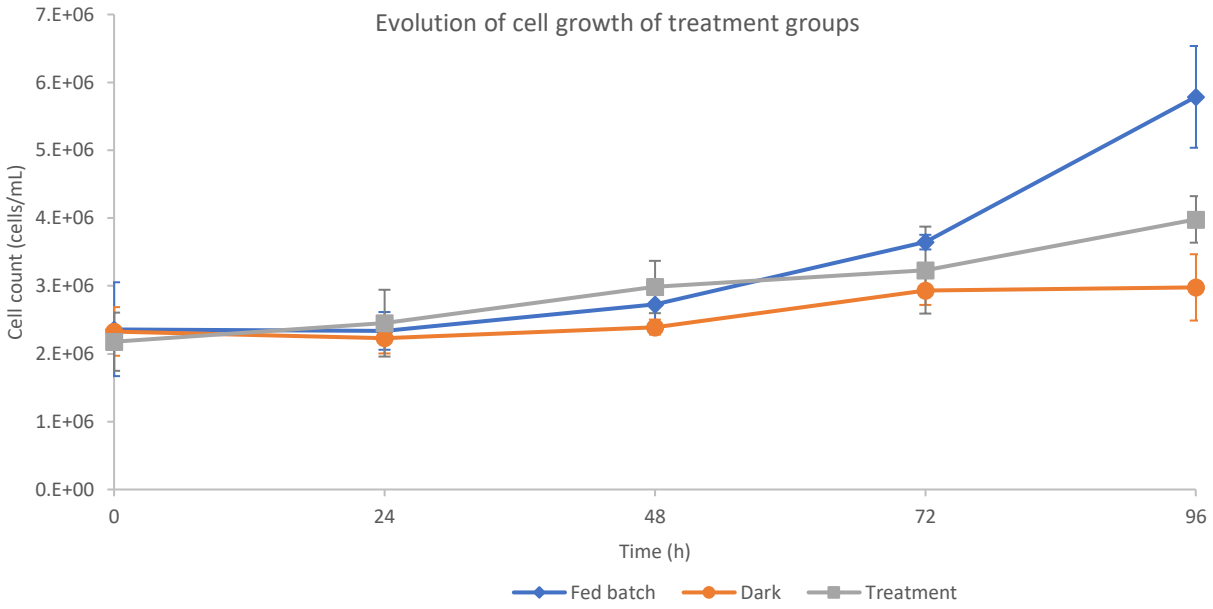

Figure 6: Evolution of cell counts in each treatment group. One data point at 96-hours was identified as outliers and removed for the single-supply group and two data points at 96-hours were identified as outliers and removed from the fed-batch group. Number of replicates varied between 3 and 6. Due to the small data set, some outliers were not removed.

As seen in **Figure 5 and 6**, the hypothetical cellular P content of cells exposed to a single P supply significantly decreased from 24- to 96-hours (t-test, p-value < 0.05) post P supply (**Figure *5***, left), while cell density increased significantly between 0 and 96-hours (, t-test, p-value < 0.05). A similar pattern was seen in the fed-batch group, as the cellular P content decreased from 24-96 hours (t-test, p-value < 0.05) post P supply (**Figure *5***, right) when cell density increased ( ). In contrast, cell density did not increase significantly from 24-96 hours in the dark group (; t-test, p-value > 0.05) and the cells did not appear to consume their cellular P content during that time (**Figure *5***, left, t-test, p-value > 0.05).

As described above, cells in the single-supply and fed-batch groups assimilated most of the P initially supplied within 24-hours (after P addition), which led to an increase of the hypothetical intracellular P content within the first 24- to 48-hours. It has been reported that PolyP consumption is associated

with cell division (Rao et al. 2009; Zachleder et al., 2016). This was observed in our experiment as cellular P content started decreasing when cell density started to increase. Cells incubated in darkness instead only partially assimilated the P initially supplied but then experienced a gradual increment in cellular P content from 24-96 hours after P addition despite not growing (T-test; p-value > 0.05). The absence of light, again, prevented the degradation of the hypothetical cellular P content for energy production (Kornberg et al., 1956; Kornberg, 1995) that would have influenced the cell density in the photosynthetic cells. PolyP storage in this case, could be essential to preserve instead of degrading for reasons not well understood yet.

3.1.3. PolyP granules quantification: Granule Counts vs Software Analysis (ImageJ)

Two methods were compared to quantify granular-PolyP degradation and verify if there was a similar trend between the visual count of granules and the software analysis:

1) the ratio of [cells with no visible granules] to [cell containing visible granules] was evaluated by manual counting of microscopic pictures. Granules were counted and scored independently of granule sizes (**Figure 19**);

2) the ratio of the [PolyP area] to [area of cells] was measured using ImageJ. The total area of the cells was first measured, followed by the total area covered by the granules. The software was manually adjusted to compute the area respectively covered by cells and granules.

The same pictures showing between 500 and 1000 cells were analysed and compared.

3.1.3.1. Single-supply group

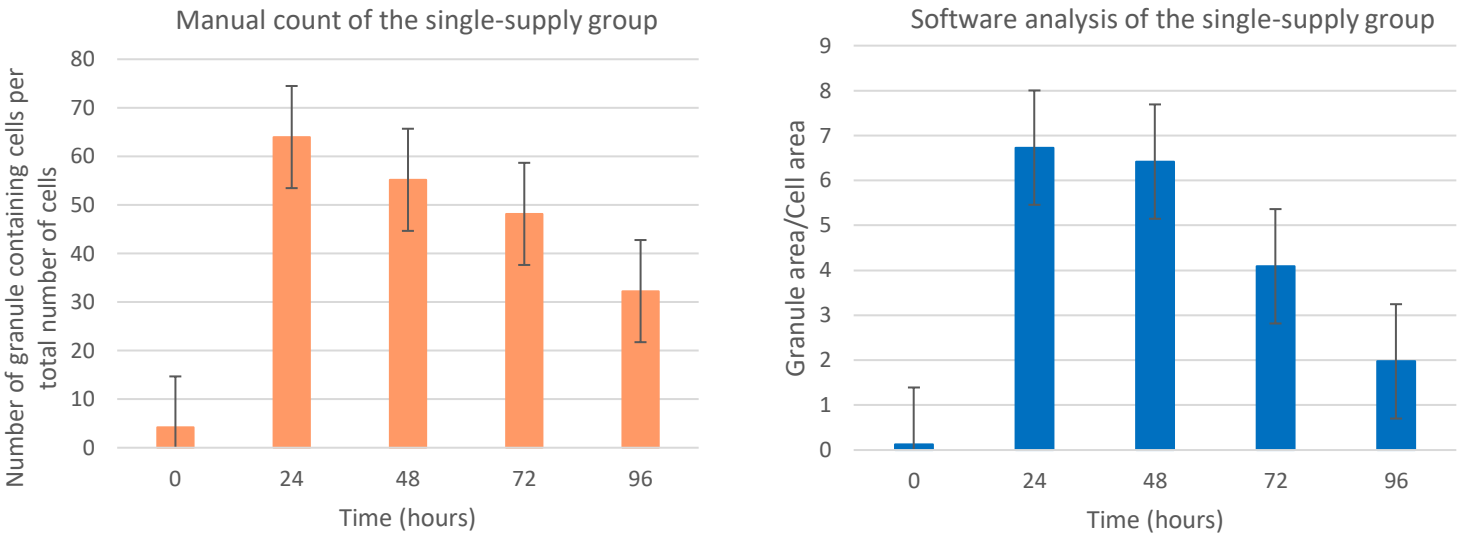

Figure 7: PolyP production and degradation analysed through manual counting of granules (left) and software analysis (right) of single-supply group.

Very few or no granules were present in the cells initially. Subsequently, the manual count and the software analysis showed the same trend: A peak at 24-hours and a slow decrease afterwards (**Figure *7***), which mirrors the trends in hypothetical cellular P content described above. As discussed previously, the consumption of the granular-PolyP (24-96 hours) was associated with an increase in cell density (**Figure *6***).

3.1.3.2. Dark group

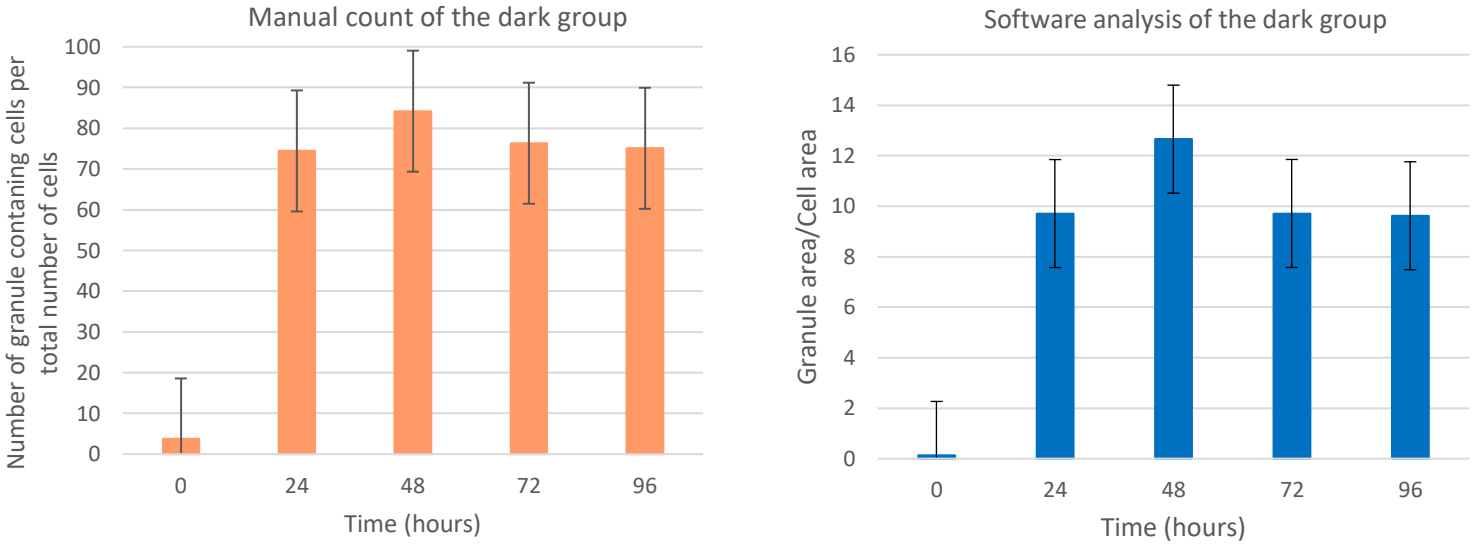

Figure 8: PolyP production and degradation trend analysed through manual count of granules (left) and software analysis (ImageJ, right) of dark group.

The manual count of PolyP granules and the software analysis in cells supplied P and incubated in the dark (**Figure *8***) again, showed a similar trend, with an observed peak at 48-hours followed but a decrease to a stable level between 72-96 hours. The initial rapid increase mirrored P content (**Figure *5***) but the hypothetical cellular content kept increasing past 24-hours when granular-PolyP content fluctuated.

3.1.3.3. *Fed-batch group*

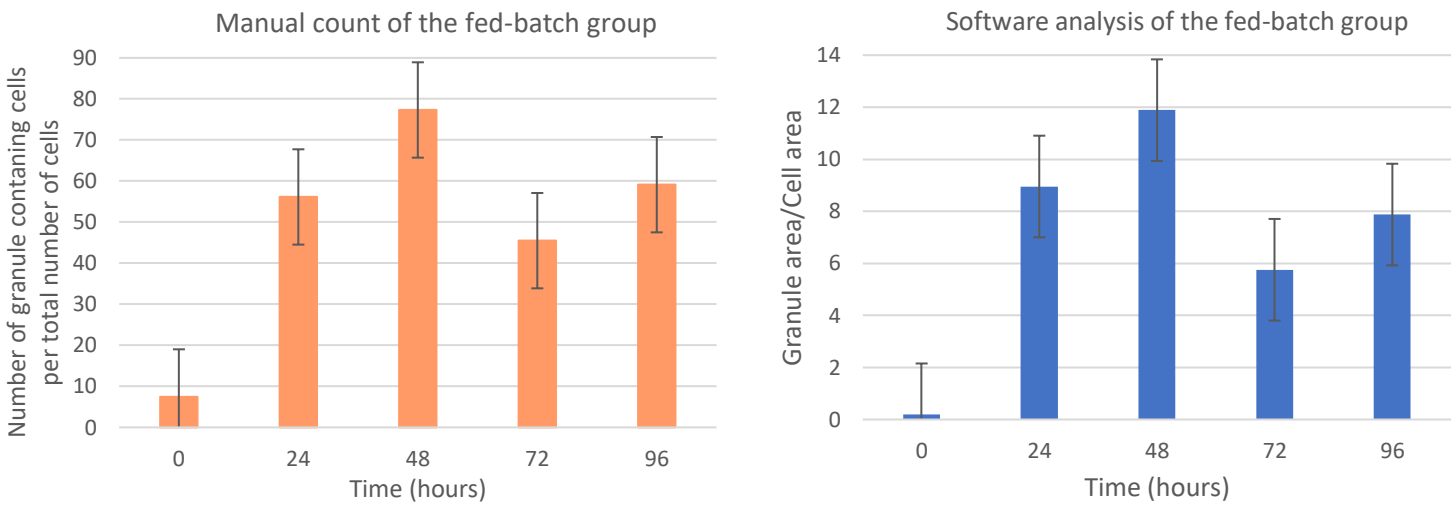

Figure 9: PolyP production and degradation analysed through manual count of granules (left) and software analysis (ImageJ, right) of fed-batch group.

As with the other treatment group, manual counting of PolyP granules and software analysis showed similar trends in the fed-batch group (**Figure *9***): The absence of granule pre-P supply followed by a rapid increase after 24-hours, a peak at 48-hours. Initially, and then a fluctuating uptake. A significant difference with the single-supply group is that the PolyP granules content remained high after 96-hours in the fed-batch group. The continued supply of phosphate may have therefore inhibited or counteracted the gradual consumption of the PolyP initially accumulated.

3.1.3.4. *Conclusions on method selection*

Similar trends were evidenced using manual counting and software analysis for the three treatment groups analysed. As software analysis was quicker and easier to perform than manual counting, consequently, only software analysis was performed in subsequent experiments.

3.2. Genetics

This section details the steps taken to select the ideal RNA extraction kit and quantification of said RNA, in addition to the quantification of gene expression of specific genes.

3.2.1. RNA extraction optimization

As stated in the literature review, we concluded that the use of column-based kits enabled higher RNA concentration and lower contamination.

- The first method tested was the Macherey-Nagel™ NucleoSpin™ RNA Plant and Fungi kit (Thermo Fisher Scientific) on 10-, 20- and 30-mL samples of *C. reinhardtii* 1690. The samples were centrifuged, the supernatant was removed, and RNA extracted according to the manufacturer's instructions. No RNA was detected in the samples after RNA extraction (below 1 ng/µL). Since the lysis buffer (containing guanidine hydrochloride) included in the kit may not have sufficiently lysed the cells, samples were transferred to NucleoSpin™ Type G Bead Tubes and homogenized using a MagNA Lyser (Roche) for 90 seconds at maximum (5,000 rpm) to aid the lysing process. This new step increased the RNA concentration in the extracts up to 38-45 ng/ µL as seen on **Table *4***. However, the RNA concentration was still low, and the samples required to be treated with DNAse.
- The second method tested was TRIzol (TIM) reagent (Thermo Fisher Scientific) and chloroform, which were directly applied to the sample, followed by RNA precipitation using isopropyl alcohol and 75% ethanol. TRIzol™ aided the breakdown of the cell wall, as it was observed under a light microscope in real time. The method provided high RNA concentration but also high contamination (**Table *4***).
- The third method tested was the PureLink RNA Mini Kit (Thermo Fisher Scientific). The lysis agent of the kit was swapped with Trizol. The column kit involves two steps that supposedly help with the breakdown of the cell wall and decrease contamination. Similarly, to the

Trizol/Chloroform method, the columns were used to remove any contaminants during the washing steps whilst providing high RNA concentration (**Table *4***).

- The last method tested was E.Z.N.A.® Plant RNA kit (Omega Bio-tek). The kit followed the same principle as the first kit tested but uses a different lysing agent (guanidine thiocyanate). The kit did not lyse the cells since the RNA concentration was very low (**Table *4***).

Table 4: Different RNA extraction kits were used to extract RNA from *C. reinhardtii* 1690 samples and analysed by NanoDrop and Qubit. The RNA concentration was measured immediately after RNA extraction (before) and after the samples were treated with DNAse (after).

Method	Sample	Qubit (before)	NanoDrop (before)	Qubit (after)	NanoDrop (after)
NucleoSpin RNA Plant and Fungi	Sample 1	38.5 ng/µL	32.2 ng/µL	35.9 ng/µL	30.8 ng/µL
NucleoSpin RNA Plant and Fungi	Sample 2	45.6 ng/µL	40.6 ng/µL	49.9 ng/µL	45.6 ng/µL
Trizol/Chloroform	Sample 1 (B)	373 ng/µL	282.6 ng/µL	249 ng/µL	312.2 ng/µL
Trizol/Chloroform	Sample 2 (C)	380 ng/µL	192.2 ng/µL	229 ng/µL	339.6 ng/µL
PureLink RNA Mini Kit (Trizol-based)	Sample 1 (B)	303 ng/µL	172.7 ng/µL	177 ng/µL	218.1 ng/µL
PureLink RNA Mini Kit (Trizol-based)	Sample 2 (C)	254 ng/µL	146.3 ng/µL	171 ng/µL	189.7 ng/µL
E.Z.N.A Plant RNA kit	Sample 1	16.1 ng/µL	14.3 ng/µL	-	-
E.Z.N.A Plant RNA kit	Sample 2	19.3 ng/µL	15.5 ng/µL	-	-

To conclude, we decided to extract RNA using the PureLink RNA Mini Kit plus Trizol. The volume of sample analysed was 10 mL. Samples were centrifuged and the supernatant was removed. RNA was extracted according to the manufacturer's instructions (ThermoFisher) with the following modifications:

- RNA was eluted in 100 µL of RNAse/DNAse-free water after RNA extraction. RNA concentration and purity were measured using Qubit and NanoDrop;
- Out of 100 µL extracted, 50 µL were removed and treated with DNAse. Treated RNA was diluted in 30 µL of RNAse/DNAse free water. RNA concentration was measured again using Qubit and NanoDrop;
- The RNA yield decreased during this process. However, we had enough sample to convert RNA to cDNA (see methods).

It was noted that there was a discrepancy between the concentrations reported by Qubit and NanoDrop. In our study, RNA concentration was measured using Qubit and NanoDrop was used to assess contamination.

3.2.2. Primer design and optimization

As mentioned earlier, seven genes were selected for analysis in this study. Of the genes selected, six are either involved in the phosphate pathway or are phosphate transporters (*vtc1*, *vtc4*, *ipy1*, *ipy3*, *ppa* and *nudix*) and one was selected as a housekeeping gene (*cblp*). The individual gene sequence was extracted from Phytozome database, and the transcript was used to design the primers using the Integrated DNA Technology (IDT) PrimerQuest Tool[2] and Geneious software's. The primers were designed over exon-intron boundaries to differentiate mRNA from possible genomic DNA contamination. The possible forward and reverse primer combinations were analysed for possible presence of hairpin-loops and primer-dimers. Two sets of primers were designed for each gene and both sets were initially tested on the cDNA of a mock sample to test their efficiency (*i.e.* two-week-old, starved *C. reinhardtii* 1690 inoculum). Samples used were detailed on **Table *5***. Primers were tested at different annealing temperatures, from 58° to 65°C, in order to identify the optimum

[2] Integrated DNA Technology (IDT) (https://sg.idtdna.com/Primerquest/Home/Index)

annealing temperature and to prevent the amplification of non-target regions. Primer pairs that performed well were both sets of *ipy1* and *ipy3* genes. Primers used for *vtc1* were selected from a previous study (Plouviez et al., 2021). Some primers yielded low gene expression in the mock sample. Therefore, we amplified the *vtc4*, *ppa* and *nudix* genes through PCR. The samples were electrophoresed on a 2% agarose gel and DNA was extracted from the gel. After DNA purification, the gel-extracted PCR product was diluted and used for qPCR analysis to check primer efficiency. Primers which failed to amplify products of the predicted size were re-designed to anneal to different intron-exon boundaries.

Table 5: Results from primer testing through PCR and 2% agarose gel. Primer efficiency was measured for the sets that were tested in further experiments. Primer sets were tested on starved *C. reinhardtii* 1690 backup inoculums.

Primer set	58°C	60°C	62°C	63°C	65°C	Efficiency[a] (1:10 dilution)
nudix 1F-1R	1 very light band	1 light band	blank	1 very light band	1 very light band	
nudix 2F-2R	2 bands	2 bands	2+ bands	Too many light bands	Too many bands	
nudix 1F2-1R	1 very light band	1 very light band	-	1 very light band	1 light band	
nudix 3F-3R	1 band	1 band	-	1 band	1 very light band	1.86 (63°C)
IPY1 1F-1R	-	1 band	-	-	-	
IPY1 2F-2R	-	1 band	-	-	-	2.072 (60°C)
IPY3 1F-1R	-	1 band	-	-	-	2.302 (60°C)
IPY3 2F-2R	-	1 band	-	-	-	
PPA 1F-1R	2 light bands	2 light bands	-	blank	blank	
PPA 2F-2R	1 band (maybe 2)	1 band	-	1 band	1 band	

PPA 3F-3R	blank	blank	-	1 light band	1 band	2.13 (63°C)
PPA 4F-4R	blank	blank	-	Several bands	Several bands	
VTC1 1F-1R	1 band	1 light band	-	1 band	1 band	1.811 (58°C)
VTC 4 1F-1R	1 dark, 1 light band	2 bands	blank	blank	blank	1.95 (63°C)
VTC 4 1F-1R2	blank	blank	-	blank	blank	
VTC 4 3F-3R	1 light band (too high)	blank	1 band (too high)	blank	1 band (too high)	
VTC 4 3F-3R2	1 light band (too high)	1 band (too high)	-	1 band (too high)	1 band (too high)	
CBLP 2F-2R		1 band	-	-	-	1.711 (58°C); 2.152 (60°C)

[a] A *good primer efficiency is between 1.8 and 2*

Following primer selection, qPCR was performed to check the gene expression of selected primer sets. The primer sets selected for further investigation were PPA (set 3), Nudix (set 3), IPY1 (set 2), IPY3 (set 1), VTC1 (set 1), VTC4 (set 1) and CBLP (set 2).

Initial analysis on duplicate samples showed that IPY1, IPY3, PPA, VTC1 and CBLP primers yielded good efficiencies (between 1.8 and 2). However, the different primer combinations and sets tested for *vtc4* and *nudix* resulted in multiple bands. This could be due to multiple amplified products, or possibly primer dimers due to the low expression of the gene of interest.

Due to these issues, only the *ipy1*, *ipy3*, *ppa*, *vtc1* and *cblp* genes were further analysed on the duplicate samples (single-supply, dark and fed-batch groups). We also analysed 'starved' samples to quantify the gene expression of the selected genes in the absence of P. For this, changes in gene expression were quantified in *C. reinhardtii* 1690 cultures deprived from external P supply for 12 days. As seen on **Table *6***, the primers showed in general a good efficiency. The *cblp* gene was amplified at a lower efficiency when tested on the same 96-well plate as the genes of interest. However, when tested alone in a single plate, the *cblp* gene was amplified at a more suitable efficiency.

Table 6: Efficiency of IPY1, IPY3, PPA, VTC1 and CBLP primers used to amplified duplicate samples (single-supply, dark and fed-batch groups) and starved samples (*C. reinhardtii* 1690 inoculum starved over a 12-day period).

	IPY1 (set 2)	IPY3 (set 1)	PPA (set 3)	VTC1 (set 1)	CBLP (set 2)
Single-supply, dark and fed-batch group	1.957 1.887	1.929	1.844 1.871	1.934	1.738
Starved samples (day 2 to 12)	1.911		1.862	1.89	1.73

3.2.3. Analysis of P-treated samples

The primer sets listed in **Table 6** were used to amplify the *ipy1*, *ipy3*, *ppa* and *vtc1* genes in duplicate samples (single-supply, dark and fed-batch) and starved samples. The RNA was amplified in the LightCycler to quantify the changes in gene expression. In cultures supplied P following a period of P depletion, duplicate cultures were incubated as described above and 10 mL samples were collected at 0-, 24-, 48-, 72- and 96-hours for RNA extraction. Starved cultures were also maintained in the incubator, and samples were extracted nearly every day for 12 days.

3.2.3.1. *Starved samples*

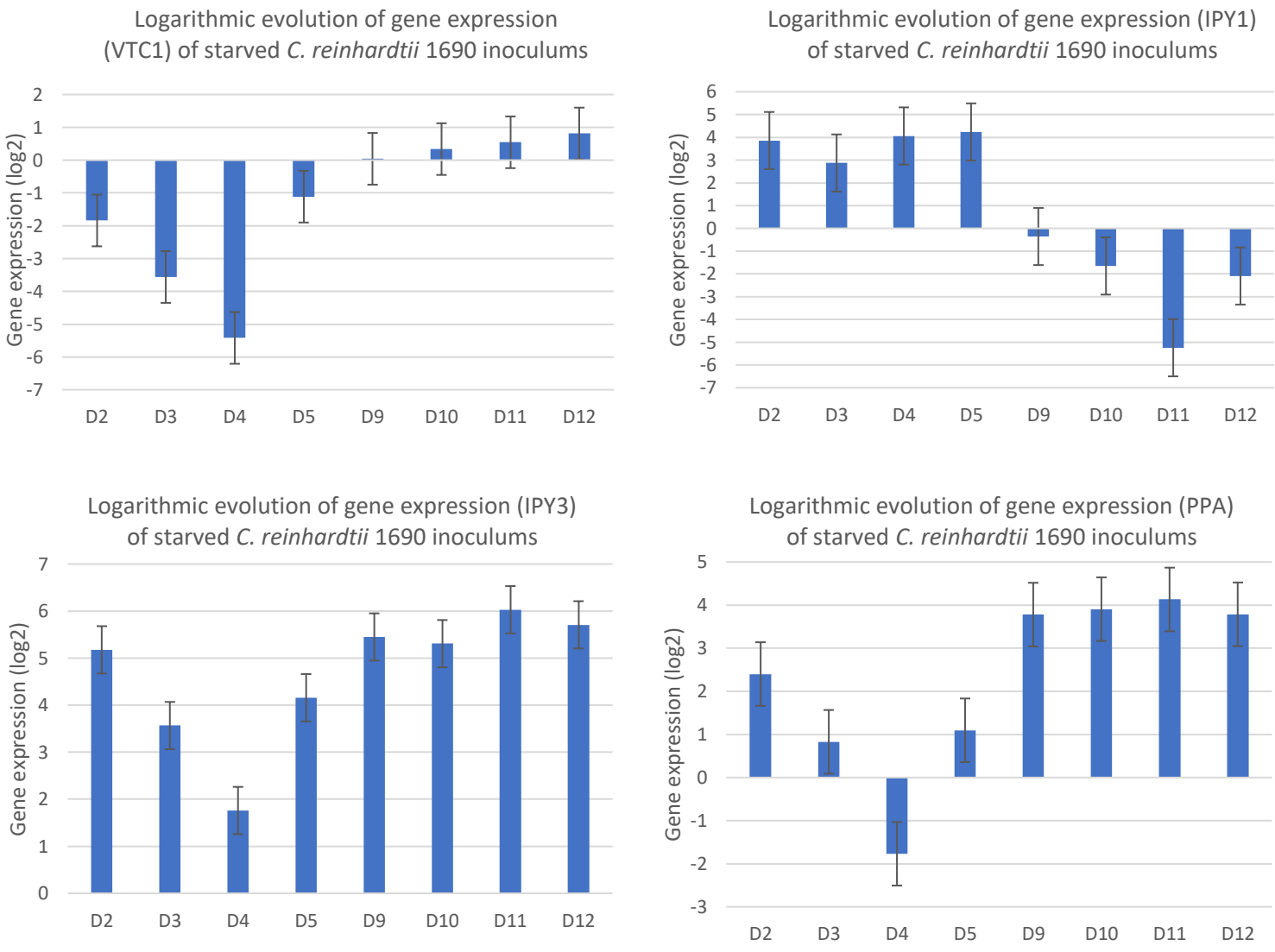

Figure 10: Quantification of expression of the *vtc1*, *ipy1*, *ipy3* and *ppa* genes in *C. reinhardtii* 1690 inoculums starved of phosphate for a period of 12 days. The Cq values* of the selected genes were normalized against the Cq values of *cblp* gene. Each sample was analysed in triplicate in the LightCycler. *the Cq (quantification cycle) value is defined by the number of cycles required to detect a fluorescent signal in the LightCycler.

As seen in **Figure *10*** (left top), *vtc1* expression was downregulated on days 2 to 5 and became upregulated after day 9. In contrast, *ipy1* expression (**Figure *10***, right top) was upregulated from days 2 to 5 but downregulated from day 9. The *ipy3* gene was upregulated during the entire

experiment, except at day 4, where its expression was temporarily downregulated (**Figure *10***, left bottom). The expression of *ppa* was upregulated throughout the experiment, except on day 4, where it was downregulated (**Figure *10***, right bottom).

Except for *ipy1*, as can be seen, all the genes studied became upregulated as P depletion likely became more severe. This could mean that *ipy3*, *ppa* and *vtc1* genes are likely upregulated under P depleted conditions. As so, they might be essential to prepare the cells for the next P supply by acting as a P starvation signal.

3.2.3.2. vtc1 expression following P supply after P depletion

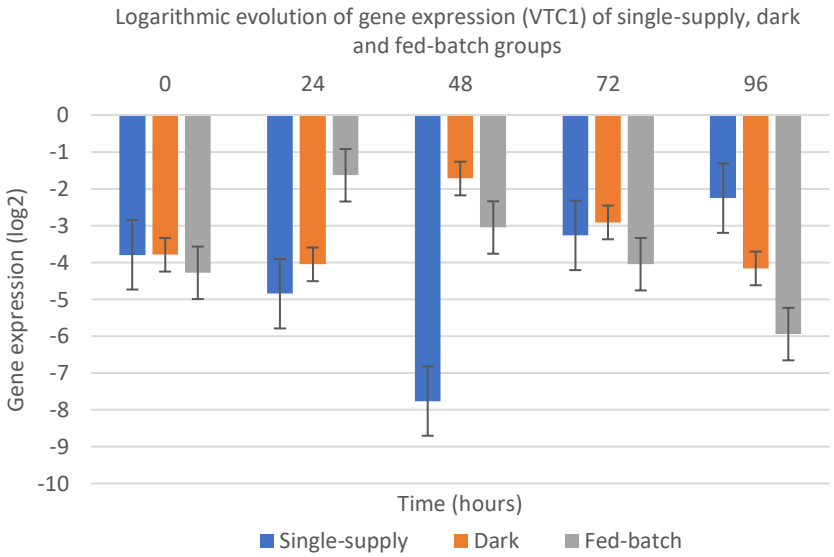

Figure 11: Changes in gene expression of *vtc1* gene in the duplicate samples (single supply, dark and fed batch) throughout a 96-hour experiment. The Cq values of *vtc1* were normalized against the Cq values of *cblp* gene. Each sample was analysed as triplicate in the LightCycler.

As seen in **Figure *11***, and although expression varied over time, *vtc1* expression was downregulated in all treatment groups throughout the entire experiment. Similar results were observed during the first five days of the starvation experiment, when *vtc1* expression was downregulated up to day five (**Figure *10***). *vtc1* is required for cell growth in the absence P (Mahmoud-Aly et al., 2018) and for the synthesis of PolyP (Hothorn et al., 2009). It was previously shown that mutants lacking the *vtc1* gene

can only thrive in P replete conditions because they are unable to produce PolyP reserves (Aksoy et al., 2014; Plouviez et al., 2021), hence we did not further analysed the role of this gene, using the mutant strain, in the degradation of PolyP. However, the gene encodes an enzyme involved in the P deplete signal responses. It is hypothesized that this gene is upregulated during P starvation to prepare the cells for the future P supply.

3.2.3.3. vtc4 expression following P supply after P depletion

We were unable to quantify the expression of *vtc4* as multiple bands persisted despite the redesign of primer sets and introduction of Dimethyl sulfoxide (DMSO). DMSO was a compound used to prevent any secondary structure from disrupting the PCR process, such as primer-dimers. We discontinued the analysis of *vtc4* gene due to possible existence of isomers, low expression, or amplification of contamination/non-target regions. However, the literature suggests that VTC4 plays an important role during P absorption and PolyP production: the VTC4 protein is required for the transport and synthesis of PolyP in yeast acidocalcisomes (Sanz-Luque et al., 2020). The VTC4 proteins in algae have functionality-related conserved residues in addition to SPX domains (Sanz-Luque et al., 2020). The small SPX domains are usually localized at the N-terminal of Pi transporters (Hurlimann et al., 2009; Hamburger et al., 2002; Liu et al., 2015; Giovannini et al., 2013), VTC complex proteins (Hothorn et al., 2009) and Pi signalling proteins (Ogawa et al., 1995; Park et al., 2014). The SPX domains bind to phosphate starvation response transcription factors to induce the expression of Pi-starvation genes under P starvation (Duan et al., 2008; Rubio et al., 2001). In addition, the SPX domain inhibits the expression of Pi-starvation genes under P-replete conditions (Puga et al., 2014; Wang et al., 2014). Due to the importance of the SPX domains, Wild and colleagues (2016) analysed mutations on the SPX domain of VTC4 protein in yeast and the effect on PolyP synthesis. They concluded that certain amino acid mutations caused the VTC4 protein to become constitutively activated during PolyP synthesis.

3.2.3.4. *ipy1 expression following P supply after P depletion*

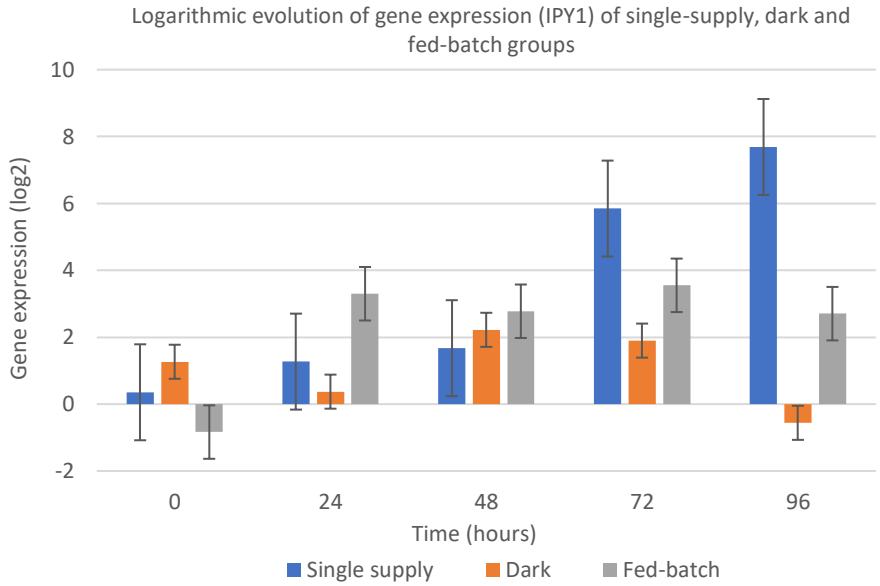

Figure 12: Changes in gene expression of *ipy1* gene in the duplicate samples (single supply, dark and fed batch) throughout a 96-hour experiment. The Cq values of *ipy1* were normalized against the Cq values of *cblp* gene. Each sample was analysed as triplicate in the LightCycler.

As seen in **Figure *12***, *ipy1* expression was low in the single-supply group immediately before P supply at 0-hours and then gradually increased throughout the experiment. The dark group also expressed the *ipy1* gene at low levels initially but, overtime, the expression kept increasing and decreasing, till it was negatively down-regulated at 96-hours. The fed-batch group presented down-regulation of the *ipy1* gene at 0-hours. In contrast to the other treatment groups, the fed-batch increased the expression rapidly within the first 24-hours. The expression fluctuated overtime.

Overall, the *ipy1* gene was expressed at low levels in all treatment groups prior to the addition of the P-shot. In the single-supply group, the expression of *ipy1* was upregulated 72-hours after P supply. In the fed-batch group, *ipy1* expression remained stable since the consumption of the PolyP initially accumulated was possibly inhibited by the continued supply of phosphate. In the dark group, *ipy1* expression fluctuated after P supply and this, unsurprisingly, was likely due to the absence of light preventing cells from producing extensive PolyP reserves and undergo cell division (Slocombe et al.,

2020). We demonstrated that the inorganic pyrophosphatase encoded by *ipy1* gene is up regulated in later stages of PolyP degradation. Although, as seen in **Figure *10***, *ipy1* is downregulated as the starvation progresses, the upregulation of *ipy1* in the later stages of PolyP degradation could a signal to initialized the P starvation responses but not necessary during P starvation.

3.2.3.5. ipy3 expression following P supply after P depletion

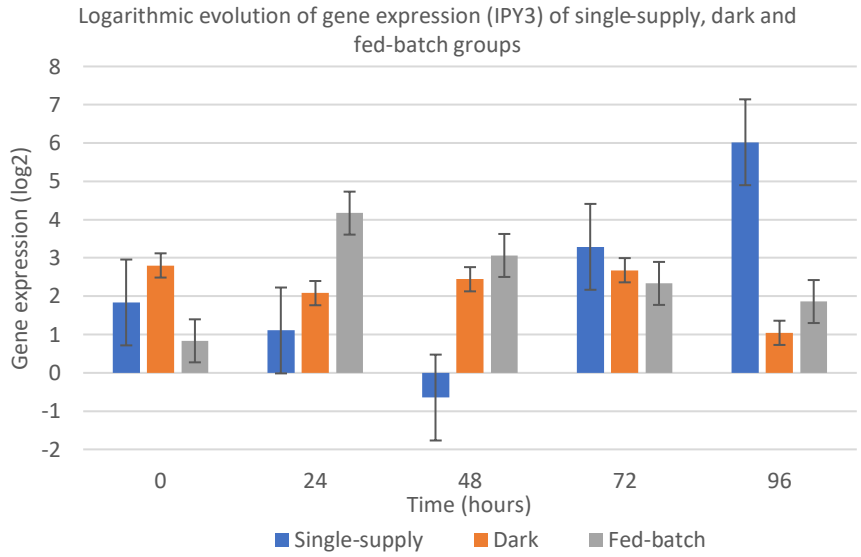

Figure 13: Changes in gene expression of *ipy3* gene in the duplicate samples (single supply, dark and fed batch) throughout a 96-hour experiment. The Cq values of *ipy3* were normalized against the Cq values of *cblp* gene. Each sample was analysed as triplicate in the LightCycler.

As seen in **Figure *13***, *ipy3* was initially upregulated prior to the addition of P-shot in all groups. This expression decreased until *ipy3* became downregulated 48-hours after P supply in the single-supply group, but this trend inverted at 72-hours and *ipy3* expression continued to increase at 96-hours. In contrast *ipy3* gene expression remained relatively stable throughout the experiment in a dark group (despite decrease in relative expression strength from 72- to 96 hours). In the fed-batch group, *ipy3* expression was upregulated initially and downregulated after 48-hours. In conclusion, the expression of *ipy3* fluctuated in the single-supply group, whilst it was more stable in the dark and fed-batch groups. The stability could be attributed to the presence of unassimilated P in the dark and fed-

batch cultures (**Figure *5***, right). I*py3*-encoded inorganic pyrophosphatase is known to cleave the shorter PolyP chains, based on our results we suggest that IPY3 has a similar function in *C. reinhardtii* and that it may be replenishing the internal Pi pool in the latter stages of PolyP degradation. In addition, it is possible that *ipy3*, similarly to *vtc1*, acts as a P starvation response for a rapid P uptake when the nutrient becomes available and remains upregulated during starvation possibly for the mobilization of the remaining reserves.

3.2.3.6. ppa expression following P supply after P depletion

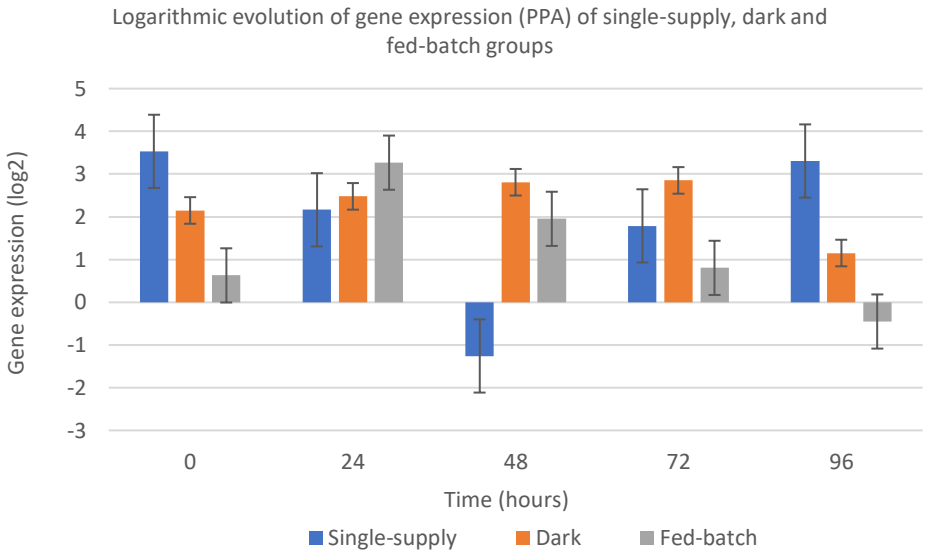

Figure 14: Changes in gene expression of *ppa* gene in the duplicate samples (single supply, dark and fed batch) throughout a 96-hour experiment. The Cq values of *ppa* were normalized against the Cq values of *cblp* gene. Each sample was analysed as triplicate in the LightCycler.

As seen in **Figure *14***, *ppa* presented variability prior to the addition of the P-shot at 0-hours. Initially, the single-supply group expressed the *ppa* gene at high levels. The expression was downregulated over 48-hours. Then, slowly, the expression started to increase at 72-hours. The dark group expressed the *ppa* gene at high levels at 0-hours. Overtime, *ppa* expression remained stable and decreased at 96-hours. Lastly, cells in the fed-batch group expressed the *ppa* gene at very low levels. However, the expression of *ppa* increased rapidly, within 24-hours, and slowly started to decrease

till it was negatively downregulated at 96-hours. We hypothesized that the inorganic pyrophosphatase family member possibly acts on short PolyP chains, similar to the *ipy3* gene, and act as a P starvation response signal and prevent further degradation of the remaining P reserves.

3.2.3.7. nudix expression following P supply after P depletion

Similar to *vtc4*, we were unable to quantify gene expression of *nudix*. The Nudix hydrolase family can be absent or present up to 26 different family members in the bacterium *Deinococcus radiodurans* (McLennan, 2006). The *S. cerevisiae* genome encodes five different Nudix hydrolases, such as Ddp1 which hydrolases diadenosine polyphosphates and diphosphoinositol polyphosphate substrates (Lawhorn et al., 2004, Klaus et al., 2005). The enzyme family is also known to be involved in the protection, regulation and signalling steps by acting as a transcriptional regulator (Ito et al., 2012). The enzymes could also reduce the intracellular levels of toxic substances (Bessman et al., 1996).

3.3. Bioassays with mutant strains

3.3.1. The analysis of bioassays of the IPY1, IPY3, PPA, Nudix and wild-type 4533 strains

Following the quantitative analysis of the *ipy1*, *ipy3*, *ppa*, and *vtc1* genes, we further analysed the potential roles of *ipy1*, *ipy3*, *ppa* and *nudix* genes using bioassays. These new experiments sought to assess if the selected mutants can produce and degrade PolyP granules throughout the experiment, using the parental wild-type 4533 strain as control. VTC1 and VTC4-knockdown mutants were not used in these assays since these mutants were previously shown not to produce granules following P supply after P depletion.

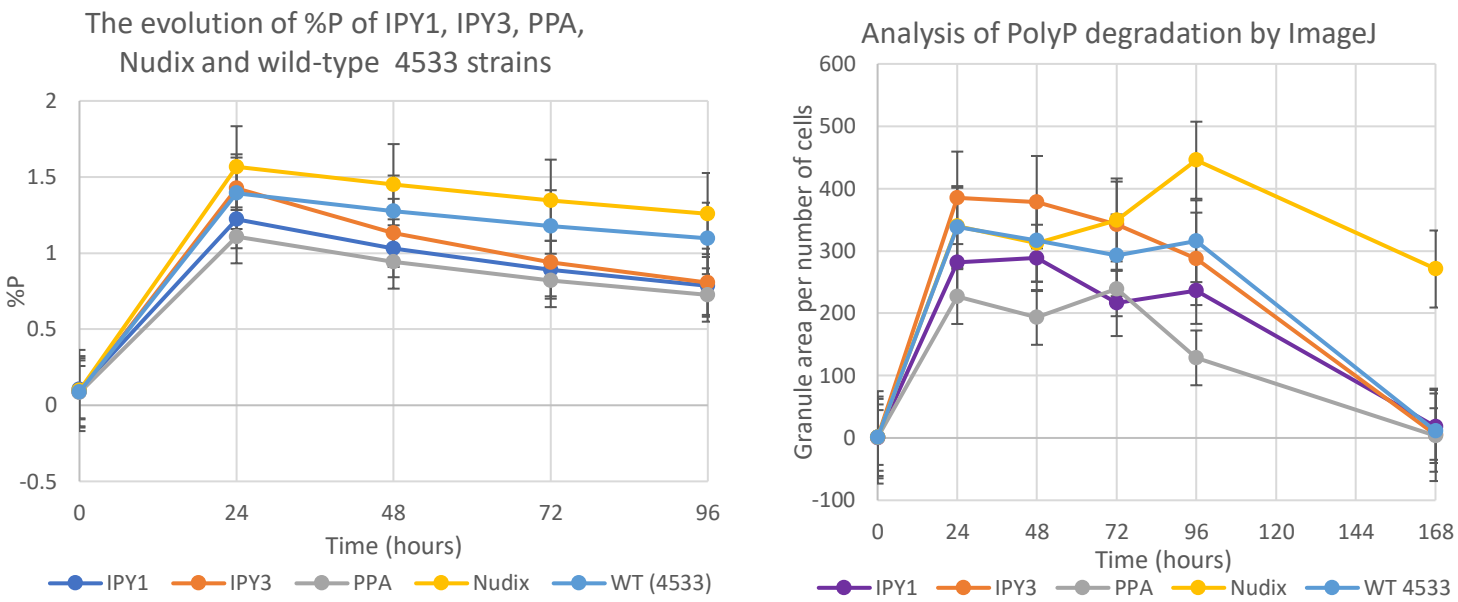

Figure 15: The evolution of the cellular P content throughout the experiment before and after the addition of the P-shot (10 mg L^{-1} P) the IPY1, IPY3, PPA, Nudix and wild-type 4533 strains (Left) (Number of replicates n = 3). The analysis of the area occupied by PolyP granules per total number of cells using ImageJ, before and after the addition of the P-shot (Right) (Number of replicates n = 10).

As seen in **Figure *17*** (Appendix), the hypothetical intracellular phosphate content of P starved strains did not significantly change throughout the experiment (reaching a peak of only 0.11 ± 0.01%). Yet, there was a significant change in the hypothetical intracellular phosphate content after the addition of P (**Figure *15***, left). At 24-hours, the %P increased up 1.39 ± 0.06% in the wild-type 4533 strain. The degradation of the PolyP granules started after 48-hours, decreasing to 1.09 ± 0.10% after 96-hours. The IPY1 mutant strain assimilated up to 1.22 ± 0.04%, which gradually decreased to 0.78 ± 0.04% after 96-hours. The IPY3 mutant strain assimilated up at 1.43 ± 0.17% at 24-hours, and throughout the experiment decreased to 0.81 ± 0.07%. The PPA mutant strain produced up to 1.11 ± 0.17% after 24-hours and slowly decreased to 0.72 ± 0.11%. The Nudix mutant strain peaked at 1.57 ± 0.01% after 24-hours, and slowly degraded to 1.26 ± 0.02%.

Overall, all the *C. reinhardtii* strains analysed quickly increased their hypothetical cellular P content in the first 24-hours, as seen previously in analysis of the *C. reinhardtii* CC-1690 (wild-type) strain.

This rapid initial uptake was followed by a slow decrease over the duration of the experiment. Depending on the strain, the cellular P content decreased by between 30 to 62% around 24- and 96-hours. Software analysis of the granular-PolyP of the IPY1, IPY3, PPA and wild-type 4533 strains revealed rapid increase followed by decrease of the quantity of PolyP granules. In contrast to the other strains, the Nudix mutant strain continued to increase its granular-PolyP. The decrease in accumulated P could be accounted for as the use of accessible P (free P_i or non-granular PolyP), rather than granular-PolyP, for cell growth. In addition, the quantity of granular-PolyP in the Nudix mutant strain was significantly higher than the other strains, where granules were no longer observed after 168-hours.

As the cellular P content of the strains analysed continued to decreased after the first 24-hours, the cell density also increased in the same time frame, except for the Nudix mutant (**Figure *16***). The IPY1, IPY3, PPA and the wild-type 4533 cell density fluctuated throughout the experiment. Overall, these strains had a positive yield whilst the Nudix mutant strain decreased in cell number after 96-hours.

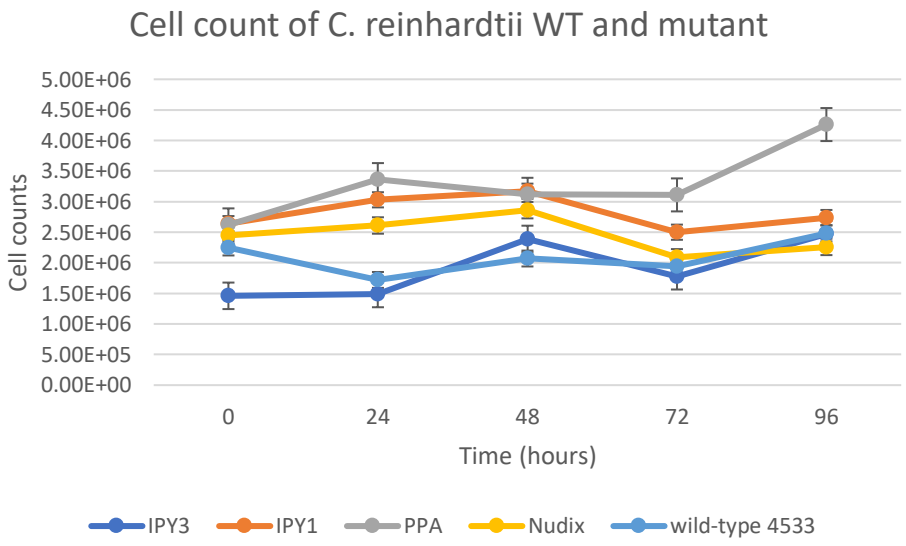

Figure 16: Cell counts of *C. reinhardtii* WT 4533 and IPY1, IPY3, PPA and Nudix mutants

As shown above, all *C. reinhardtii* strains analysed assimilated P, leading to the synthesis of granular-PolyP and increase in %P. The strains initially behaved similarly; however, significant changes were visualized 168-hours (7 days) after the P-shot: Nearly all granular-PolyP had disappeared in the wild-type 4533, IPY1, IPY3 and PPA mutant cells after 7 days, as so we concluded that *ip1*, *ipy3* and *ppa* genes do not encode a PolyP degrading enzyme, or that other enzymes with similar functions were activated to compensate for the absentee gene. Diaz and colleagues (2005) showed that the absence of PPK enzymes led to the overexpression of *pst* genes in *Streptomyces lividans* to maintain normal cell activities. We nevertheless demonstrated that the absence of *ipy1*, *ipy3* and *ppa* genes does not inhibit the degradation of granular-PolyP in *C. reinhardtii* strains.

In the Nudix mutant, on the other hand, granular-PolyP degradation was considerably slower, and growth was inhibited (**Figure *16***). Previously, similar events have been reported such as in *Dictyostelium discoideum* PPK1 mutants, where half of the mutant cells failed to divide due to the mutation (Zhang et al., 2007). We therefore hypothesised that the *nudix* gene encodes an enzyme involved in the degradation of PolyP for cell growth, which was inhibited in the mutant strain, preventing the release of energy from PolyP. However, as we can see in **Figure *15*** (right), the granular-PolyP decreased from 96 to 168-hours. This suggests that the cells possibly utilized another energy source (nitrogen) for cell division, which instead of consuming the granular-PolyP, the reservoirs were divided between the daughter cells. However, we did not verify if, indeed, the cells increased in number between 96 and 168-hours.

3.4. Conclusions

In this study, we established a reproducible protocol for the analysis of the degradation of PolyP in *C. reinhardtii* strains. We quantified the expression of *vtc1*, *ipy1*, *ipy3*, and *ppa* genes through P depletion and repletion phases. To explore the possible implications of changes in expression associated with changes in PolyP intracellular concentration, we tested the ability of IPY1, IPY3, PPA and Nudix mutants to synthesize and degrade PolyP. We previously could only assume that genes formerly analysed in other microorganisms, could be present and involved in the degradation of PolyP in *C. reinhardtii*. However, after this study we provided evidence that the *nudix* gene likely encodes an enzyme involved in the consumption of granular-PolyP in *C. reinhardtii*. In conclusion, the *nudix* gene presented promising results and a step closer to a better knowledge of PolyP consumption in the model species *C. reinhardtii*.

3.5. Future prospects

This thesis aimed to identify enzymes involved in the intracellular consumption of granular-PolyP granules in *C. reinhardtii* with the analysis of different wild type and mutant strains. Through the analysis of IPY1, IPY3, PPA and Nudix mutant strains, we concluded that *nudix* gene encodes an enzyme with a relevant role in the degradation process. The *vtc4* and *nudix* genes were analysed with different sets and combinations of our current designed primers, however multiple sets of products were amplified. The ambiguous results could be due to contamination/non-target regions amplification, but also to the differential splicing of the genes or to uncharacterized genes with similar sequences. As stated in the literature review, one single species (*Deinococcus radiodurans*) could possess up to 26 different Nudix genes. Ideally, we will optimize the primers and the amplicons produced during qPCR will be sequenced and further analysed.

As stated in the literature review, the Nudix hydrolases 2 and 4 were involved in the degradation of short and long PolyP chains in *T. brucei*. However, it is unknown if the *C. reinhardtii* Nudix enzyme can degrade long or short PolyP chains. To test this hypothesis, biochemical assays should be used to test the activity of the enzyme on PolyP chains of different lengths as done by Cordeiro et al. (2019), since it is unknown the specific preference of the Nudix enzyme of *C. reinhardtii*.

As stated in the results/discussion section, the absorption of dissolved P of the dark group was not complete. Unbeknownst why, we suggest resuspending the cells in P-free media after 48-hours to verify if the rather elevated presence of dissolved P could be preventing the cells from initiating P starvation responses. The dark group, opposed to the other two, continued to uptake P intracellularly and failed to go through the process of cell division.

And lastly, as stated in the literature review, different triggers may influence the degradation of PolyP. Experiments could be designed to investigate how the triggers, such as cadmium, sulphur, mercury and ammonium affect the degradation of PolyP in *C. reinhardtii*.

Section 4: References

Achbergerová, L. & Nahálka, J (2011). Polyphosphate – an ancient energy source and active metabolic regulator. *Microbial Cell Factories*, 10 (63), 1-14

Adhya, T. K., Kumar, N., Reddy, G., Podile, A. R., Bee, H. & Samantaray, B. (2015). Microbial mobilization of soil phosphorus and sustainable P management in agricultural soils. *Current Science*, 108 (7), 1280-1287

Aguilera, A. & Amils, R. (2005). Tolerance to cadmium in *Chlamydomonas* sp. (Chlorophyta) strains isolated from an extreme acidic environment, the Tinto River (SW, Spain). *Aquatic Toxicology*, 75 (4), 316-329

Ahn, K. & Kornberg, A. (1990). Polyphosphate kinase from *Escherichia coli* - Purification and demonstration of a phosphoenzyme intermediate. *Journal of Biological Chemistry*, 265 (20), 11734–11739

Aitchison, P. A. & Butt, V. S. (1973). The relation between the synthesis of inorganic polyphosphate and phosphate uptake by *Chlorella vulgaris*. *Journal of Experimental Botany*, 24 (3), 497-510

Akiyama, M., Crooke, E. & Kornberg, A. (1992). The polyphosphate kinase gene *of Escherichia coli* - Isolation and sequence of the *ppk* gene and membrane location of the protein. *Journal of Biological Chemistry*, 267 (31), 22556-22561

Akiyama, M., Crooke, E. & Kornberg, A. (1993). An exopolyphosphatase of *Escherichia coli* - The enzyme and its *ppx* gene in a polyphosphate operon. *Journal of Biological Chemistry*, 268 (1), 633-639

Aksoy, M., Pootakham, W. & Grossman, A. R. (2014). Critical function of a *Chlamydomonas reinhardtii* putative polyphosphate polymerase subunit during nutrient deprivation. *Plant Cell*, 26 (10), 4214-4229

Andreeva, N. A., Kulakovskaya, T. V. & Kulaev, I. S. (1998). Purification and properties of exopolyphosphatase isolated from *Saccharomyces cerevisiae* vacuoles. *FEBS Letters*, 429 (2), 194–196

Andreeva, N. A., Kulakovskaya, T. V. & Kulaev, I. S. (2006). High molecular mass exopolyphosphatase from the cytosol of the yeast *Saccharomyces cerevisiae* is encoded by the *PPN1* gene. *Biochemistry – Moscow*, 71 (9), 975–977

Andreeva, N., Trilisenko, L., Eldarov, M. & Kulakovskaya, T. (2015). Polyphosphate *PPN1* of *Saccharomyces cerevisiae:* Switching of exopolyphosphatase and endopolyphosphatase activities. *PLOS One*, 10 (3), 1-11

Archibald, F. S. & Fridovich, I. (1982). Investigations of the state of the manganese in *Lactobacillus plantarum*. *Archives of Biochemistry and Biophysics*, 215 (2), 589-596

Arezi, B., Xing, W. M., Sorge, J.A. & Hogrefe, H.H. (2003). Amplification efficiency of thermostable DNA polymerases. *Analytical Biochemistry*, 321 (2), 226–235

Baykov, A. A., Cooperman, B. S., Goldman, A. & Lahti, R. (1999). Cytoplasmic inorganic pyrophosphatase. *Inorganic Polyphosphates*, 23, 127–150

Bennett, M., Onnebo, S. M., Azevedo, C., & Saiardi, A. (2006) Inositol pyrophosphates: metabolism and signalling. *Cell and Molecular Life Sciences*, 63 (5), 552–564

Bessman, M. J., Frick, D. N. & O'Handley, S. F. (1996). The MutT proteins or "Nudix" hydrolases, a family of versatile, widely distributed, "housecleaning" enzymes. *Journal of Biological Chemistry*, 271 (41), 25059-25062

Blum, E., Py, B., Carpousis, A. J. & Higgins, C. F. (1997). Polyphosphate kinase is a component of the *Escherichia coli* RNA degradosome. *Molecular Microbiology*, 26 (2), 387-398

Bourke, W., Bilby, S., Hamilton, D. & McDowell, R. (2005). Recent water improvement initiatives using melter slag materials. New Zealand Wastewater Association Publications, EnviroNZ05 Conference, Auckland, New Zealand, 28-30, September 2005

Bolier, G., de Koningh, M, C. J., Schmale, J. C. & Donze, M. (1992). Differential luxury phosphate response of planktonic algae to phosphorus removal. *Hydrobiologia*, 243, 113-118

Brown, N. & Shilton, A. (2014). Luxury uptake of phosphorus by microalgae in waste stabilisation ponds: current understanding and future direction. *Reviews in Environmental Science and Bio/Technology*, 13 (3), 321-328

Burton, A., Hu, X., & Saiardi, A. (2009) Are inositol pyrophosphates signalling molecules? Journal of *Cellular Physiology*, 220 (1), 8–15

Castuma, C. E., Huang, R., Kornberg, A. & Reusch, R.N. (1995). Inorganic polyphosphates in the acquisition of competence in *Escherichia coli*. *Journal of Biological Chemistry*, 270 (22), 12980-12983

Cembella, A. D., Antia, N. J. & Harrison, P. J. (1984a). The utilization of inorganic and organic phosphorus compounds as nutrients by eukaryotic microalgae - a multidisciplinary perspective: part 1. *Critical Reviews in Microbiology*, 10 (4), 317-391

Cembella, A. D., Antia, N. J. & Harrison, P. J. (1984b). The utilization of inorganic and organic phosphorus compounds as nutrients by eukaryotic microalgae - a multidisciplinary perspective: part 2. *Critical Reviews in Microbiology*, 11 (1), 13–81

Chislock, M. F., Doster, E., Zitomer, R. A. & Wilson, A. E. (2013). *Eutrophication: causes, consequences and controls in aquatic ecosystems*. The nature education knowledge project. Retrieved from https://www.nature.com/scitable/knowledge/library/eutrophication-causes-consequences-and-controls-in-aquatic-102364466/

Chomczynski, P. & Sacchi, N. (1987). Single-step method of RNA isolation by acid guanidinium thiocyanate-phenol chloroform extraction. *Analytical Biochemistry*, 162 (1), 156–159

Cohen, A., Perzov, N., Nelson, H. & Nelson, N. (1999). A novel family of yeast chaperons involved in the distribution of V-ATPase and other membrane proteins. *Journal of Biological Chemistry*, 274 (38), 26885-26893

Cooperman, B.S., Baykov, A.A. & Lahti, R. (1992) Evolutionary conservation of the active site of soluble inorganic pyrophosphatase. *Trends Biochemistry Science*, 17 (7), 262–266

Cordeiro, C. D., Ahmed, M. A., Windle, B. & DoCampo, R. (2019). NUDIX hydrolases with inorganic polyphosphate exo- and endophosphatase activities in the glycosome, cytosol and nucleus of *Trypanosoma brucei*. *Bioscience Reports*, 39 (5), 1-11

Cordell, D., Drangert, J-O. & White, S (2009). The story of phosphorus: Global food security and food for thought. *Global Environmental Change – Human and Policy Dimensions*, 19 (2), 292-305

Cordell, D. & White, S. (2011). Peak phosphorus: clarifying the key issues of a vigorous debate about long-term phosphorus security. *Sustainability*, 3 (10), 2027-2049

Crimp, A., Brown, N. & Shilton, A. (2018). Microalgal luxury uptake of phosphorus in waste stabilization ponds – frequency of occurrence and high performing genera. *Water Science and Technology*, 78 (1), 165-173

Curtis, T. P., Mara, D. D. & Silva, S. A. (1992). Influence of pH, oxygen, and humic substances on ability of sunlight to damage fecal coliforms in waste stabilization pond water. *Applied and Environmental Microbiology*, 58 (4), 1335-1343

de Jesus, T. C. L., Tonelli, R. R., Nardelli, S. C., Augusto, L. S., Motta, M. C. M., Girard-Dias, W., Miranda, K., Ulrich, P., Jimenez, V., Barquilla, A., Navarro, M., DoCampo, R. & Schenkman, S. (2010). Target of rapamycin (TOR)-like 1 kinase is involved in the control of polyphosphate levels and acidocalcisome maintenance in *Trypanosoma brucei*. *Journal of Biological Chemistry*, 285 (31), 24131-24140

Desfougères, Y., Gerasimaitė, R., Jessen, H. J. & Mayer, A. (2016). Vtc5, a Novel Subunit of the Vacuolar Transporter Chaperone Complex, Regulates Polyphosphate Synthesis and Phosphate Homeostasis in Yeast. *Journal of Biological Chemistry*, 291 (42), 22262-22275

Diaz, M., Esteban, A., Fernandez-Abalos, J. M. & Santamaria, R. I. (2005). The high-affinity phosphate-binding protein PstS is accumulated under high fructose concentrations and mutation of the corresponding gene affects differentiation in *Streptomyces lividans*. *Microbiology-SGM*, 151 (8), 2583–2592

DoCampo, R., Jimenez, V., King-Keller, S., Li, Z-H. & Moreno, S. N. J. (2011). The role of acidocalcisomes in the stress response of *Trypanosoma cruzi*. In Weiss, L. M., Tanowitz, H. B. & Kirchnoff, L.V. (Eds.), Advances in Parasitology, Vol 75: Changas Disease, PT A (307-324)

DoCampo, R. & Huang, G. (2016). Acidocalcisomes of eukaryotes. *Current Opinion in Cell Biology*, 41, 66-72

Dove, S. K., McEwen, R. K., Mayes, A., Hughes, D. C., Beggs, J. D. & Michell, R. H. (2002). Vac14 controls PtdIns (3,5) P-2 synthesis and Fab1-dependent protein trafficking to the multivesicular body. *Current Biology*, 12 (11), 885-893

Downey, M. (2019). A stringent analysis of polyphosphate dynamics in *Escherichia coli*. *Journal of Bacteriology*, 201 (9), 1-6

Duan, K., Yi, K. K., Dang, L., Huang, H. J., Wu, W. & Wu, P. (2008). Characterization of a sub-family of Arabidopsis genes with the SPX domain reveals their diverse functions in plant tolerance to phosphorus starvation. *Plant Journal*, 54 (6), 965-975

EcoSanRes, 2008. *Closing the Loop on Phosphorus*. Stockholm Environment Institute (SEI) funded by SIDA Stockholm. Retrieved from http://www.ecosanres.org/pdf_files/ESR-factsheet-04.pdf

Elser, J. & Bennet, E. (2011). A broken biogeochemical cycle. *Nature*, 478 (7367), 29-31

Garcia, J., Mujeriego, R., Bourrouet, A., Penuelas, G. & Freixes, A. (2000). Wastewater treatment by pond systems: experiences in Catalonia, Spain. *Water Science and Technology*, 42 (10), 35-42

Fang, J. M., Rohloff, P., Miranda, K. & DoCampo, R. (2007). Ablation of a small transmembrane protein of *Trypanosoma brucei* (TbVTC1) involved in the synthesis of polyphosphate alters acidocalcisome biogenesis and function and leads to a cytokinesis defect. *Biochemical Journal*, 407, 161-170

Gerasimaitė, R., Sharma, S., Desfougères, Y., Schmidt, A. & Mayer, A. (2014). Coupled synthesis and translocation restrains polyphosphate to acidocalcisomes-like vacuoles and prevents its toxicity. *Journal of Cell Science*, 127 (23), 5093-5104

Giovannini, D., Touhami, J., Charnet, P., Sitbon, M. & Battini, J. L. (2013). Inorganic Phosphate Export by the Retrovirus Receptor XPR1 in Metazoans. *Cell Reports*, 3 (6), 1866-1873

Gomez-Garcia, M. R., Losada, M. & Serrano, A. (2007). Comparative biochemical and functional studies of family I soluble inorganic pyrophosphatases from photosynthetic bacteria. *FEBS Journal*, 274 (15), 3948-3959

Goodenough, U., Heiss, A. A., Roth, R., Rusch, J. & Lee, J. H. (2019). Acidocalcisomes: Ultrastructure, biogenesis and distribution in microbial eukaryotes. *Protist*, 170 (3), 287-313

Gray, M. J. & Jakob, U. (2015). Oxidative stress protection by polyphosphate— new roles for an old player. *Current Opinion in Microbiology*, 24, 1–6

Güsewell, S. (2004). N:P ratios in terrestrial plants: variation and functional significance. *New Phytologist*, 164 (2), 243-266

Hamburger, D., Rezzonico, E., Petetot, J. M. C., Somerville, C. & Poirier, Y. (2002). Identification and characterization of the Arabidopsis *PHO1* gene involved in phosphate loading to the xylem. *Plant Cell*, 14 (4), 889-902

Harold, F. M. (1966). Inorganic polyphosphate in biology – structure metabolism and function. *Bacteriological Reviews*, 30 (4), 772-794

Hothorn, M., Neumann, H., Lenherr, E .D., Wehner, M., Rybin, V., Hassa, P. O., Uttenweiler, A., Reinhardt, M., Schmidt, A., Seiler, J., Ladurner, A. G., Herrmann, C., Scheffzek, K. & Mayer, A. (2009). Catalytic core of a membrane-associated eukaryotic polyphosphate polymerase. *Science*, 324 (5926), 513–516

Higuchi, R., Fockler, C., Dollinger, G. & Watson, R. (1993). Kinetics PCR analysis – real-time monitoring of DNA amplification reactions. *Bio-Technology*, 11 (9), 1026-1030

Huh, W. K., Falvo, J. V., Gerke, L. C., Carroll, A. S., Howson, R. W., Weissman, J. S. & O'Shea, E. K. (2003). Global analysis of protein localization in budding yeast. *Nature*, 425 (6959), 686-691

Hurlimann, H. C., Pinson, B., Stadler-Waibel, M., Zeeman, S. C. & Freimoser, F. M. (2009). The SPX domain of the yeast low-affinity phosphate transporter Pho90 regulates transport activity. *EMBO Reports*, 10 (9), 1003-1008

Ishige, K., Zhang, H. Y. & Kornberg, A (2002). Polyphosphate kinase (PPK2), a potent, polyphosphate-driven generator of GTP. *Proceedings of the National Academy of Sciences of the United States of America*, 99 (26), 16684-16688

Ito, D., Kato, T., Maruta, T., Tamoi, M., Yoshimura, K. & Shigeoka, S. (2012). Enzymatic and Molecular Characterization of Arabidopsis ppGpp Pyrophosphohydrolase, AtNUDX26. *Bioscience Biotechnology and Biochemistry*, 76 (12), 2236-2241

Jiménez, J., Bru, S., Ribeiro, M. P. C. & Clotet, J. (2016). Polyphosphate: popping up from oblivion. *Current Genetics*, 63 (1), 15-18

Kasprak, A. (2016). The desert rock that feeds the world. The Atlantic. Retrieved from https://www.theatlantic.com/science/archive/2016/11/the-desert-rock-that-feeds-the-world/508853/

Keasling, J. D. (1997). Regulation of intracellular toxic metals and other cations by hydrolysis of polyphosphate. *Bioremediation of Surface and Subsurface Contamination*, 829, 242-249

Klaus, S. M. J., Wegkamp, A., Sybesma, W., Hugenholtz, J., Gregory, J. F. & Hanson, A. D. (2005). A nudix enzyme removes pyrophosphate from dihydroneopterin triphosphate in the folate synthesis pathway of bacteria and plants. *Journal of Biological Chemistry*, 280 (7), 5274-5280

Kornberg, A., Kornberg, S. R. & Simms, E. S. (1956). Metaphosphate synthesis by an enzyme from *Escherichia-coli*. *Biochimica et Biophysica acta*, 20 (1), 215-227

Kornberg, A. (1995). Inorganic polyphosphate – toward making a forgotten polymer unforgettable. *Journal of Bacteriology*, 177 (3), 491-496

Kornberg, A., Rao, N. N. & Ault-Riche, D. (1999). Inorganic polyphosphate: a molecule of many functions. *Annual Review of Biochemistry*, 68, 89-125

Kuang, J. J., Yan, X., Genders, A. J., Granata, C. & Bishop, D. J. (2018). An overview of technical considerations when using quantitative real-time PCR analysis of gene expression in human exercise research. *PLOS ONE*, 13 (5), 1-27

Kulaev, I. S. (1975). Biochemistry of inorganic polyphosphates. *Reviews of Physiology Biochemistry and Pharmacology*, 73, 131-158

Kulaev, I. S. & Vagabov, V. M. (1983). Polyphosphate metabolism in micro-organisms. *Advances in Microbial Physiology*, 24, 83-171

Kulakovskaya, T. V., Andreeva, N. A. & Kulaev, I. S. (1997). Adenosine-5'-tetraphosphate and guanosine-5'-tetraphosphate: new substrates of the cytosolic exopolyphosphatase of the yeast Saccharomyces cerevisiae. *Biochemistry – Moscow*, 62 (9), 1051-1052

Kulakovskaya, T. V., Trilisenko, L. V., Lichko, L. P., Vagabov, V. M. & Kulaev, I. S. (2006). The effect of inactivation of the exo- and endopolyphosphatase genes PPX1 and PPN1 on the level of different polyphosphates in the yeast *Saccharomyces cerevisiae*. *Microbiology*, 75 (1), 25-28

Kuroda, A. & Kornberg, A. (1997). Polyphosphate kinase as a nucleoside diphosphate kinase in *Escherichia coli* and *Pseudomonas aeruginosa*. *Proceedings of the National Academy of Sciences of the United States of America*, 94 (2), 439-442

Lander, N., Ulrich, P. N. & DoCampo, R. (2013). *Trypanosoma brucei* vacuolar transporter chaperone 4 (TbVtc4) is an acidocalcisome polyphosphate kinase required for in vivo infection. *Journal of Biological Chemistry*, 288 (47), 34205-34216

Lawhorn, B. G., Gerdes, S. Y. & Begley, T. P. (2004). A genetic screen for the identification of thiamin metabolic genes. *Journal of Biological Chemistry*, 279 (42), 43555-43559

Lemercier, G., Dutoya, S., Luo, S. H., Ruiz, F. A., Rodrigues, C. O., Baltz, T., DoCampo, R. & Bakalara, N. (2002). A vacuolar-type H-pyrophosphatase governs maintenance of functional acidocalcisomes and growth of the insect and mammalian forms of *Trypanosoma brucei*. *Journal of Biological Chemistry*, 277 (40), 37369-37376

Li, Z-H., Alvarez, V. E., De Gaudenzi, J. G., Sant'Anna, C., Frasch, A. C. C., Cazzulo, J. J. & DoCampo, R. (2011). Hyperosmotic stress induces aquaporin-dependent cell shrinkage, polyphosphate synthesis, amino acid accumulation, and global gene expression changes in *Trypanosoma cruzi*. *Journal of Biological Chemistry,* 286 (51), 43959-43971

Lichko, L., Kulakovskaya, T., Pestov, N. & Kulaev, I. (2006). Inorganic polyphosphates and exopolyphosphatases in cell compartments of the yeast *Saccharomyces cerevisiae* under inactivation of *PPX1* and *PPN1* genes. *Bioscience Reports*, 26 (1), 45-54

Lichko, L. P., Kulakovskaya, T. V., Kulakovskaya, E. V. & Kulaev, I. S. (2008). Inactivation of *PPX1* and *PPN1* genes encoding exopolyphosphatases of *Saccharomyces cerevisiae* does not prevent utilization of polyphosphates as phosphate reserve. *Biochemistry (Moscow)*, 73 (9), 985-989

Liu, J. L., Yang, L., Luan, M. D., Wang, Y., Zhang, C., Zhang, B., Shi, J. S., Zhao, F. G., Lan, W. Z. & Luan, S. (2015). A vacuolar phosphate transporter essential for phosphate homeostasis in Arabidopsis. *Proceedings of the National Academy of Sciences of the United States of America*, 112 (47), E6571-E6578

Lonetti, A., Szijgyarto, Z., Bosch, D., Loss, O., Azevedo, C. & Saiardi, A. (2011). Identification of an evolutionarily conserved family of inorganic polyphosphate endopolyphosphatases. *Journal of Biological Chemistry*, 286 (37), 31966– 31974

Lundin, M., Baltscheffsky, H. & Ronne, H. (1991). Yeast *PPA2* gene encodes a mitochondrial inorganic pyrophosphatase that is essential for mitochondrial function. *The Journal of Biological Chemistry*, 266 (19), 12168–12172

MacDonald, G. K., Bennet, E. M., Potter, P. A. & Ramankutty, N. (2011). Agronomic phosphorus imbalances across the world's croplands. *Proceedings of the National Academy of Sciences of the United States of America*, 108 (7), 3086-3091

Macfie, S. M., Tarmohamed, Y. & Welbourn, P. M. (1994). Effects of cadmium, cobalt, copper and nickel on the growth of the green alga *Chlamydomonas reinhardtii:* the influences of the cell wall and pH. *Archives of Environmental Contamination and Toxicology*, 27 (4), 454-458

Mahmoud-Aly, M., Li, Y., Shanab, S. M. M., Amin, A. Y. & Ahmed, A. H. H. (2018). Physiological characterization of a *Chlamydomonas reinhardtii vacuolar transporter chaperon 1* mutant under phosphorus deprivation condition. *Bioscience Research*, 15 (4), 4532-4539

Matile, P. (1978). Biochemistry and function of vacuoles. *Annual Review of Plant Physiology and Plant Molecular Biology*, 29, 193–213

McLennan, A. G. (2006). The Nudix hydrolase superfamily. *Cellular and Molecular Life Sciences*, 63 (2), 123-143

Michelet, L., Zaffagnini, M., Vanacker, H., Le Marechal, P., Marchand, C., Shroda, M., Lemaire, S. D. & Decottignies, P. (2008). *In vivo* targets of s-thiolation in *Chlamydomonas reinhardtii*. *The Journal of Biological Chemistry*, 231 (31), 21571-21578

Mining Technology (2016). *What's shaping the future of phosphorus?* Mining Technology. Retrieved from https://www.mining-technology.com/features/featurephosphorus-whats-shaping-the-future-of-this-vital-element-4913074/

Moreno, S. N. J. & Docampo, R. (2013). Polyphosphate and Its Diverse Functions in Host Cells and Pathogens. *PLoS Pathogens*, 9 (5), 1-3

Mullis, K. B. & Faloona, F. A. (1987). Specific synthesis of DNA in vitro via a polymerase-catalyzed chain reaction. *Methods in Enzymology,* 155, 335-350

Müller, O., Bayer, M. J., Peters, C., Andersen, J. S., Mann, M. & Mayer, A. (2002). The Vtc proteins in vacuole fusion: coupling NSF activity to V-0 trans-complex formation. *EMBO Journal*, 21 (3), 259-269

Müller, O., Neumann, H., Bayer, M.J. & Mayer, A. (2003). Role of the Vtc proteins in V-ATPase stability and membrane trafficking. *Journal of Cell Science*, 116 (6), 1107-1115

Nahalka, J. & Patoprsty, V. (2009). Enzymatic synthesis of sialylation substrates powered by a novel polyphosphate kinase (PPK3). *Organic & Biomolecular Chemistry*, 7 (9), 1778-1780

Negreiros, R.S, Lander, N., Huang, G., Cordeiro, C.D, Smith, S.A, Morrissey, J.H & DoCampo, R. (2018) Inorganic polyphosphate interacts with nucleolar and glycosomal proteins in trypanosomatids. *Molecular Microbiology*, 110 (6), 973–994

Nishikawa, K., Yamakoshi, Y., Uemura, I. & Tominaga, N. (2003). Ultrastructural changes in *Chlamydomonas acidophila* (Chlorophyta) induced by heavy metals and polyphosphate metabolism. *FEMS Microbiology Ecology*, 44 (2), 253-259

Nishikawa, K., Machida, H., Yamakoshi, Y., Ohtomo, R., Saito, K., Saito, M. & Tominaga, N. (2006). Polyphosphate metabolism in an acidophilic alga *Chlamydomonas acidophila* KT-1 (Chlorophyta) under phosphate stress. *Plant Science*, 170 (2), 307-313

NZIER (2012). *Economic impact of Chatham Rock Phosphate*. NZIER, authoritative analysis. Retrieved from: https://nzier.org.nz/static/media/filer_public/9b/7d/9b7d0cd5-3aa2-4817-8035-71dfea3ab60f/economic_impact_of_crp.pdf

NZIER (2014). *Economic impact of Chatham Rock Phosphate: Input to the environmental impact assessment.* NZIER New Zealand Institute of Economic Research. Retrieved from https://www.epa.govt.nz/assets/FileAPI/proposal/EEZ000006/Applicants-proposal-documents/2e35d7bdef/EEZ000006-Appendix06-NZIER-CRP-Economic-effects-of-Chatham-Rock-Phosphate-Mar-2014.pdf

Ogawa, N., Noguchi, K., Sawai, H., Yamashita, Y., Yompakdee, C. & Oshima, Y. (1995). Functional domains of Pho81p, an inhibitor of Pho85p protein kinase, in the transduction pathway of Pi signals in *Saccharomyces cerevisiae*. *Molecular Cell Biology*, 15 (2), 997-1004

Ogawa, N., DeRisi, J. & Brown, P.O. (2000). New components of a system for phosphate accumulation and polyphosphate metabolism in *Saccharomyces cerevisiae* revealed by genomic expression analysis. *Molecular Biology of the Cell*, 11 (12), 4309-4321

Onnebo, S. M. N. & Saiardi, A. (2009). Inositol pyrophosphates modulate hydrogen peroxide signalling. *Biochemical Journal*, 423, 109-118

Park, B. S., Seo, J. S. & Chua, N. H. (2014). NITROGEN LIMITATION ADAPTATION Recruits PHOSPHATE2 to Target the Phosphate Transporter PT2 for Degradation during the Regulation of Arabidopsis Phosphate Homeostasis. *Plant Cell*, 26 (1), 454-464

Pick, U. & Weiss, M. (1991). Polyphosphate hydrolysis within acidic vacuoles in response to amine-induced alkaline stress in the halotolerant alga *Dunaliella-salina*. *Plant Physiology*, 97 (3), 1234-1240

Plouviez, M; Fernandez, E; Grossman, R. A; Sanz-Luque, E; Sells, M; Wheeler, D; Guieysse, B. (2021) Responses of *Chlamydomonas reinhardtii* during the transition from P-deficient to P-sufficient growth (the P-overplus response): the roles of the vacuolar transport chaperones and polyphosphate synthesis. *Journal of Phycology*. In press.

Powell, N., Shilton, A., Chisti, Y. & Pratt, S. (2009). Towards a luxury uptake process via microalgae – defining the polyphosphate dynamics. *Water Research*, 43 (17), 4207-4213

Powell, N., Shilton, A., Pratt, S. & Chisti, Y. (2011). Luxury uptake of phosphorus by microalgae in full scale waste stabilization ponds. *Water Science and Technology*, 63 (4), 704-709

Pratt, C., Shilton, A., Pratt, S., Haverkamp, R. G. & Elmetri, I. (2007). Effects of redox potential and pH changes on phosphorus retention by melter slag filters treating wastewater. *Environmental Science and Technology*, 41 (18), 6585-6590

Puga, M. I., Mateos, I., Charukesi, R., Wang, Z., Franco-Zorrilla, J. M., de Lorenzo, L., Irigoye, M. L., Masiero, S., Bustos, R., Rodriguez, J., Leyva, A., Rubio, V., Sommer, H. & Paz-Ares, J. (2014). SPX1 is a phosphate-dependent inhibitor of PHOSPHATE STARVATION RESPONSE 1 in Arabidopsis. *Proceedings of the National Academy of Sciences of the United States of America*, 111 (41), 14947-14952

Purzycka, J.K., Olewiecki, I., Soltyszewski, I., Pepinski, W. & Janica, J. (2006). Efficiency comparison of seven different Taq polymerases used in hemogenetics. *International Congress Series*, 1288, 719–721

Rao, N. N. & Knorberg, A. (1996). Polyphosphate supports resistance and survival of stationary-phase *Escherichia coli*. *Journal of Bacteriology*, 178 (5), 1394-1400

Rao, N. N., Liu, S. J. & Kornberg, A. (1998). Inorganic polyphosphate in *Escherichia coli*: the phosphate regulon and the stringent response. *Journal of Bacteriology*, 180 (8), 2186-2193

Rao, N. N., Gomez-Garcia, M. R. & Kornberg, A. (2009). Inorganic polyphosphate: essential for growth and survival. *Annual Review of Biochemistry*, 78, 605-647

Ray, K., Mukherjee, C. & Ghosh, A. N. (2013). A way to curb phosphorus toxicity in the environment: use of polyphosphate reservoir of cyanobacteria and microalga as a safe alternative phosphorus biofertilizer for Indian agricultural. *Environmental Science and Technology*, 47 (20), 11378-11379

Rhee, G.-Y. (1973). A continuous culture study of phosphate uptake, growth rate and polyphosphate in *Scenedesmus* sp. *Journal of Phycology*, 9 (4), 495–506

Rose, P. & Dunn, K. (2013). A high rate ponding unit operation linking treatment of tannery effluent and *Arthrospira* (Spirulina) biomass production. 1: Process development. *Biomass and Bioenergy*, 51, 183-188

Roser, M., Ritchie, H. & Ortiz-Ospina, E. (2019). World population growth. Our World in Data. Retrieved from https://ourworldindata.org/world-population-growth

Rosmarin, A., 2004. *The Precarious Geopolitics of Phosphorous*. Down to Earth. Retrieved from https://www.downtoearth.org.in/coverage/the-precarious-geopolitics-of-phosphorous-11390

Rubio, V., Linhares, F., Solano, R., Martin, A. C., Iglesias, J., Leyva, A. & Paz-Ares, J. (2001). A conserved MYB transcription factor involved in phosphate starvation signalling both in vascular plants and in unicellular algae. *Genes and Development*, 15 (16), 2122-2233

Ruiz, F. A., Marchesini, N., Seufferheld, M., Govindjee & DoCampo, R. (2001). The Polyphosphate bodies of *Chlamydomonas reinhardtii* possess a Proton-pumping pyrophosphatase and are similar to acidocalcisomes. *Journal of Biological Chemistry*, 276 (49), 46196-46203

Ruiz-Martinez, A., Serralta, J., Pachés, M., Seco, A. & Ferrer, J. (2014). Mixed microalgae culture for ammonium removal in the absence of phosphorus: effect of phosphorus supplementation and process modelling. *Process Biochemistry*, 49 (12), 2249-2257

Safrany, S. T., Caffrey, J. J., Yang, X. N., Bembenek, M. E., Moyer, M. B., Burkhart, W. A. & Shears, S. B. (1998). A novel context for the 'MutT' module, a guardian of cell integrity, in a diphosphoinositol polyphosphate phosphohydrolase. *EMBO Journal*, 17 (22), 6599-6607

Samadani, M. & Dewez, D. (2018). Effect of mercury on the polyphosphate level of alga *Chlamydomonas reinhardtii*. *Environmental Pollution*, 240, 506-513

Sanz-Luque, E., Bhaya, D. and Grossman, A. R. (2020). Polyphosphate: A Multifunctional Metabolite in Cyanobacteria and Algae. *Frontiers in Plant Science*, 11 (938), 1-21

Scholz, R. W. & Wellmer, F-W. (2013). Approaching a dynamic view on the availability of mineral resources: what we may learn from the case of phosphorus? *Global Environmental Change*, 23 (1), 11-27

Sells, M. D., Brown, N. & Shilton, A. N. (2018). Determining variables that influence the phosphorus content of waste stabilization pond algae. *Water Research*, 132, 301-308

Serodio, J., Cartaxana, P., Coelho, H. & Vieira, S. (2009). Effects of chorophyll fluorescence on the estimation of microphytobenthos biomass using spectral reflectance indices. *Remote Sensing of Environment*, 113 (8), 1760-1768

Sethuraman, A., Rao, N. N. & Kornberg, A. (2001). The endopolyphosphatase gene: essential in *Saccharomyces cerevisiae*. *Proceedings of the National Academy of Sciences of the United States of America*, 98 (15), 8542–8547

Sharpley, A. N., Withers, P. J. A., Abdalla, C. W. & Dodd, A. R., (2005). Strategies for the Sustainable Management of Phosphorus. In J. T. Sims & A. N. Sharpley (Eds.). Phosphorus: Agriculture and the Environment (379-414). American Society of Agronomy

Shears, S. B. (2009) Diphosphoinositol Polyphosphates: Metabolic Messengers? *Molecular Pharmacology*, 76 (2), 236–252

Shi, X. & Kornberg, A. (2005). Endopolyphosphatase in *Saccharomyces cerevisiae* undergoes post-translational activations to produce short-chain polyphosphates. *FEBS Letters*, 579 (9), 2014–2018

Shintani, T., Uchiumi, T., Yonezawa, T., Salminen, A., Baykov, A.A., Lahti, R. & Hachimori, A. (1998) Cloning and expression of a unique inorganic pyrophosphatase from *Bacillus subtilis*: evidence for a new family of enzymes. *FEBS Letters*, 439 (3), 263–266

Slocombe, S. P., Zúñiga-Burgos, T., Chu, L., Wood, N. J., Camargo-Valero, M. A. & Baker, A. (2020). Fixing the broken phosphorus cycle: wastewater remediation by microalgal polyphosphates. *Frontiers in Plant Science*, 11 (982), 1-17

Smil, V., 2000. Phosphorus in the environment: natural flows and human interferences. *Annual Review of Energy and the Environment,* 25, 53–88

Solovchenko, A., Verschoor, A. M., Jablonowski, N. D. & Nedbal, L. (2016). Phosphorus from wastewater to crops: an alternative path involving microalgae. *Biotechnology Advances*, 34 (5), 550-564

Solovchenko, A., Khozin-Goldberg, I., Selyakh, I., Semenova, L., Ismagulova, T., Lukyanov, A., Mamedov, I., Vinogradova, E., Karpova, O., Konyukhov, I., Vasilieva, S., Mojzes, P., Dijkema, C.,

Song, Y. S., Kang, C., Jeong, J., Kim, K-O. & Lim, E. (2018). Rheological analysis of live and dead microalgae suspensions. *Journal of the Korean Physical Society*, 72 (8), 858-862

Steen, I., 1998. Phosphorus availability in the 21st Century: management of a non-renewable resource. *Phosphorus and Potassium*, 217, 1-13

Tesena, P., Korchunjit, W., Taylor, J. & Wongtawan, T. (2017). Comparison of commercial RNA extraction kits and qPCR master mixes for studying gene expression in small biopsy tissue samples from the equine gastric epithelium. *Journal of Equine Science*, 28 (4), 135-141

Tsutsumi, K., Munekata, M. & Shiba, T. (2000). Involvement of inorganic polyphosphate in expression of SOS genes. *Biochimica et Biophysica Acta-Gene Structure and Expression*, 1493 (1-2), 73-81

Uttenweiler, A., Schwarz, H., Neumann, H. & Mayer, A. (2007). The vacuolar transporter chaperone (VTC) complex is required for microautophagy. *Molecular Biology of the Cell*, 18 (1), 166-175

Valledor, L., Furuhashi, T., Hanak, A-M. & Weckwerth, W. (2013). Systemic cold stress adaptation of *Chlamydomonas reinhardtii. Molecular & Cellular Proteomics*, 12 (8), 2032-2047

Van Veen, H. W., Abee, T., Kortstee, G. J. J., Konings, W. N. & Zehnder, A. J. B. (1994a). Translocation of metal phosphate via the phosphate inorganic transport system of *Escherichia coli*. *Biochemistry*, 33 (7), 1766-1770

Van Veen, H. W., Abee, T., Kortstee, G. J. J., Pereira, H., Konings, W. N. & Zehnder, A. J. B. (1994b). Generation of a proton motive force by the extraction of metal-phosphate in the polyphosphate-accumulating *Acinetobacter johnsonii* strain 210A. *Journal of Biological Chemistry*, 269 (47), 29509-29514

Wang, Z. Y., Ruan, W. Y., Shi, J., Zhang, L., Xiang, D., Yang, C., Li, C. Y., Wu, Z. C., Liu, Y., Yu, Y. A., Shou, H. X., Mo, X. R., Mao, C. Z. & Wu, P. (2014). Rice SPX1 and SPX2 inhibit phosphate starvation responses through interacting with PHR2 in a phosphate-dependent manner. *Proceedings of the National Academy of Sciences of the United States of America*, 111 (41), 14953-14958

Wang, L., Yan, J., Wise, M. J., Liu, Q., Asenso, J., Huang, Y., Dai, S., Liu, Z., Du, Y. & Tang, D. (2018). Distribution patterns of polyphosphate metabolism pathway and its relationships with bacterial durability and virulence. *Frontiers in Microbiology*, 9 (782), 1-10

Werner, T. P., Amrhein, N. & Freimoser, F. M. (2007). Specific localization of inorganic polyphosphate (poly P) in fungal cell walls by selective extraction and immunohistochemistry. *Fungal Genetics and Biology*, 44 (9), 845-852

Wichern, M., Gehring, T. & Lübken, M. (2018). Modeling of biological systems in wastewater treatment. *Reference Module in Earth Systems and Environmental Sciences*

Wild, R., Gerasimaite, R., Jung, J-Y., Truffault, V., Pavlovic, I., Schmidt, A., Saiardi, A., Jessen, H.J., Poirier, Y., Hothorn, M. & Mayer, A. (2016). Control of eukaryotic phosphate homeostasis by inositol polyphosphate sensor domains. *Science*, 352 (6288), 986–990

Wood, H. G. & Clark, J. E. (1988). Biological aspects of inorganic polyphosphates. *Annual Review of Biochemistry*, 57, 253-260

Yang, X., Wu, X., Hao, H-L. & He, Z-L. (2008). Mechanism and assessment of water eutrophication. *Journal of Zhejiang University-Science B*, 9 (3),197-209

Young, T.W., Kuhn, N.J., Wadeson, A., Ward, S., Burges, D. & Cooke, G.D. (1998) *Bacillus subtilis* ORF yybQ encodes a manganese-dependent inorganic pyrophosphatase with distinctive properties: the first of a new class of soluble pyrophosphatase? *Microbiology*, 144 (9), 2563–2571

Zachleder, V., Bisova, K., and Vitova, M. (2016). The Cell Cycle of Microalgae. In M. A. Borowitzka, J. Beardall and J. A. Raven (Eds.), The Physiology of Microalgae (3–46), Springer

Zhang, H., Gomez-Garcia, M. R., Shi, X., Rao, N. N. & Kornberg, A. (2007). Polyphosphate kinase 1, a conserved bacterial enzyme, in a eukaryote, Dictyostelium discoideum, with a role in cytokinesis. *Proceedings of the National Academy of Sciences of the Unites States of America*, 104 (42), 16486–16491

Section 5: Appendix

3.6. MM low-P and Ammonia acetate low-P media recipe

Table 7: Minimal media recipe.

Minimal Media – low phosphate	Volume (1000 mL)
Macronutrient solution	10 mL
$CaCl_2 \cdot 2H_2O$	5 g/ 100 mL
$MgSO_4 \cdot 7H_2O$	10 g/ 100 mL
$NaNO_3$	31.7 g/ 500 mL
Phosphate solution (31 mg-P·L^{-1})	32 µL
K_2HPO_4	115 g/ 100 mL
KH_2PO_4	46 g/ 100 mL
Trace elements	1 mL
EDTA	25 g/ 500 mL
BO_3H_3	5.7 g/ 500 mL
$ZnSO_4 \cdot 7H_2O$	11 g/ 500 mL
$MnCl_2 \cdot 6H_2O$	2.55 g/ 500 mL
$FeSO_4 \cdot 7H_2O$	2.50 g/ 500 mL
$CoCl_2 \cdot 6H_2O$	0.80 g/ 500 mL
$CuSO_4 \cdot 5H_2O$	0.80 g/ 500 mL
$MoO_4Na_2 \cdot 2H_2O$	107 mg/ 500 mL

Table 8: Ammonium acetate low phosphate media recipe.

Ammonium acetate low phosphate media	Volume (1000 mL)
Stock solution of Trizma base	20 mL
Trizma base	12.1 g/ 100 mL
Stock solution of nutrient solution (NH_4^+)	10 mL
$CaCl_2 \cdot 2H_2O$	5 g/ 100 mL
$MgSO_4 \cdot 7H_2O$	10 g/ 100 mL
NH_4Cl	4 g/ 100 mL
Stock solution of phosphate solution (31 mg-P·L^{-1})	32 µL
K_2HPO_4	115 g/ 100 mL
KH_2PO_4	46 g/ 100 mL
Trace elements	1 mL
EDTA	25 g/ 500 mL
BO_3H_3	5.7 g/ 500 mL
$ZnSO_4 \cdot 7H_2O$	11 g/ 500 mL
$MnCl_2 \cdot 6H_2O$	2.55 g/ 500 mL
FeSO4·7H2O	2.50 g/ 500 mL
CoCl2·$6H_2O$	0.80 g/ 500 mL
$CuSO_4 \cdot 5H_2O$	0.80 g/ 500 mL
$MoO_4Na_2 \cdot 2H_2O$	107 mg/ 500 mL
Acetic acid	800 µL
CH_3COOH	99% pure

3.7. Accession number of selected genes

The sequences of the selected genes were extracted from Phytozome database (www.phytozome.net) under the following accession numbers: *vtc1* (Cre12.g510250), *vtc4* (Cre02.g140700), *ipy1* (Cre10.g424100), *ipy3* (Cre09.g387875), *ppa* (Cre06.g390200) and *nudix hydrolase* (Cre02.g106500).

3.8. RNA extraction (Trizol™ Plus RNA Puri cation Kit)

As stated on the manufacturer guide:

- 1 mL of Trizol™ Reagent was added per 100 mg of cell pellet. Samples were vortexed during incubation for 5 minutes at room temperature.
- Chloroform was added (0.2 mL/1 mL of Trizol™ Reagent) to aid cell lysis and the samples were manually mixed for 2-3 minutes at room temperature.
- Centrifuge the sample for 15 minutes at 12,000 g at 4°C and transfer, approximately, 600 µL of colourless upper aqueous phase to a clean 1.5 mL microtube. Add equal volume of 70% ethanol to sample, followed by vortex.
- Transfer 700 µL of sample to a spin cartridge (with collection tube). Centrifuge at 12,000 x g for 1 minute, remove supernatant and re-use collection tube.
- Transfer remaining sample to spin cartridge and repeat steps above.
- After all sample was transferred to spin cartridge, centrifuge tube to remove excess ethanol still present in the column. Replace old collection tube with a new one.
- Wash spin cartridge with 700 µL of Wash Buffer I and centrifuge at 12,000 x g for 1 minute. Remove supernatant and re-use collection tube during wash steps.
- Wash spin cartridge with 500 µL of Wash Buffer II and centrifuge at 12,000 x g for 1 minute. Repeat previous step again with Wash Buffer II.
- Lastly, centrifuge spin cartridge at 12,000 x g for 1 minute to remove excess ethanol.
- Place spin column into a clean RNAse-free 1.5 mL microtube. Add 100 µL RNAse-free water into spin cartridge and centrifuge at 12,000 x g for 2 minutes. Pipet supernatant containing RNA, and transfer sample to spin column again and centrifuge at 12,000 x g for 2 minutes. Discard spin column.

3.8.1. DNAse treatment

For this purpose, 50 µL of the 100 µL of RNA extracted was transferred to a clean 1.5 mL microtube and completed with 10 µL DNAse Buffer, 39 µL RNAse-free water and 1 µL DNAse. Warm sample at 37ºC for 10 minutes in heating pad. Add 1 volume (10 µL) of 3 M NaOAc pH 5.0 and 2.5 volumes (250 µL) of EtOH (absolute) and place sample at -80ºC for 1 hour. Remove sample from freezer and centrifuge for 15 minutes at 12,000 x g. Discard supernatant and wash tube with 500 µL of 70% EtOH. Centrifuged for 10 minutes at 12,000 x g. Remove supernatant. Dry pellet at 37ºC until ethanol evaporates and re-suspended pellet in 30-50 µL RNAse-free water.

3.9. RNA concentration

3.9.1. Qubit (ThermoFisher)

Firstly, Qubit master mix was produced depending of number of samples. Add 199 µL x n (number of samples) of Qubit RNA BR Buffer and 1 µL x n of Qubit RNA BR Reagent to a 2 mL microtube, mix well. To produce standards, transfer 190 µL of master mix to 2 Qubit tubes, and 10 µL of Qubit RNA BR standard 1 (0 ng/µL) and 2 (100 ng/µL). Transfer 197 µL of master mix to Qubit tubes and 3 µL of sample.

3.10. Reverse transcriptase

3.10.1. qScript™ XLT cDNA SuperMix

Place qScript XLT cDNA SuperMix (5x) on ice and prepare samples in a RNase/DNase-free fumehood. Transfer qScript XLT cDNA SuperMix (5x) and water to 0.2 mL microtubes (**Table *9***) and close them prior to leaving fumehood. Transfer RNA samples to microtubes. The variable volume is dependent of the RNA concentration, in this experiment, we aimed to produce up to 500 ng/µL.

Table 9: Components for a convertion of RNA to cDNA with qScript XLT cDNA SuperMix (5x).

Component	Volume (µL)	Final concentration
qScript XLT cDNA SuperMix (5x)	4	1x
RNA template	Variable	Between 2 µg to 10 pg total RNA
RNase/DNase-free water	Variable	-
Total	20	-

Vortex samples briefly to mix contents. Transfer 0.2 mL microtubes to PCR machine. Incubate samples for 5 minutes at 25°C, 60 minutes at 42°C, 5 minutes at 85°C and hold samples at 10°C.

3.11. PCR amplification

3.11.1. EmeraldAmp GT PCR Master Mix (2x)

Place EmeraldAmp GT PCR Master Mix (2x) on ice and prepare samples in a RNase/DNase-free fumehood. Transfer EmeraldAmp GT PCR Master Mix (2x), water, forward and reverse primers to a 0.2 mL microtube (**Table *10***) and close them prior to leaving fumehood. Prepare negative control by excluding cDNA sample. Dilute cDNA samples for PCR/qPCR amplification. Dilution used in this study was 1/5. Transfer cDNA samples to microtubes on a clean RNase/DNase-free lab bench.

Table 10: PCR amplification master mix with EmeraldAmp GT PCR Master Mix (2x).

Components	Volume (µL)	Final concentration
EmeraldAmp GT PCR Master Mix (2x)	10	1x
Forward Primer	1	-
Reverse Primer	1	-
RNase/DNase-free water	6	-
Template	2	1/5 dilution
Total	20	-

Vortex samples briefly to mix contents. Transfer 0.2 mL microtubes to PCR machine. The PCR program followed as stated in **Table *11***.

Table 11: Steps of a PCR cycle.

Step	Temperature (ºC)	Time	
Initial denaturing	94ºC	3 minutes	-
Denaturing	94ºC	30 seconds	-
Annealing	Variable	30 seconds	T(ºC) depends on primers
Elongation	72ºC	Variable	15 seconds for every 500 bp
Final elongation	72ºC	5 minutes	-

3.12. qPCR amplification in a LightCycler 480

Remove 5x HOT FIREPol SolisGreen qPCR Mix from the freezer to ice and prepare samples in a RNase/DNase-free fumehood. Transfer 5x HOT FIREPol SolisGreen qPCR Mix, water, forward and reverse primers master mix to a 0.2-1 mL centrifuge tube, depending on number of samples (as stated on **Table *12***). Transfer 8 µL of qPCR master mix to the negative wells of a 96 well qPCR plate. Then close negative control samples with sticky tape to prevent contamination. Transfer 8 µL of qPCR master mix to the other wells. Surround plate with sticky tape while moving to a clean RNase/DNase-free lab bench. Transfer 2 µL of cDNA samples (1/10 dilution) to the correct wells, excluding the negative control. Finally remove all sticky tape and cover the plate with sealing foil provided with the kit. Plate was centrifuged at 3000x g for 20 seconds. Cover plate with aluminium foil, till LightCycler 480 was ready to analyse samples.

Table 12: Components of a qPCR reaction with 5x HOT FIREPol SolisGreen qPCR Mix.

Components	Volume (µL)	
RNase/DNase-free water	5	Half of mix volume
5x HOT FIREPol SolisGreen qPCR Mix	2	
Forward primer	0.5	
Reverse primer	0.5	
cDNA template	2	Diluted to 1/10
Total	10	

The 96-well plate was inserted in the LightCycler 480 and the program used for all samples was detailed on **Table *13***. Annealing temperature (*) varied depending on the primer set analysed.

Table 13: Amplification program in LightCycler 480. *temperature depends on the annealing temperature of the primer set used.

Program	Temperature	Acquisition Mode	Time	Cycles	Analysis Mode
Pre-incubation				1	None
	95°C	None	00:10:00		
Amplification				40	Quantification
	95°C	None	00:00:10		
	60 °C*	None	00:00:20		
	72 °C	Single	00:00:20		
Melting Curve				1	Melting Curves
	95 °C	None	00:00:05		
	65 °C	None	00:01:00		
	97 °C	Continuous			
Cooling				1	None
	40 °C	None	00:00:30		

3.12.1. Analysis of LightCycler 480 results

Data was extracted from LightCycler as a text file. The text file was analysed in the program LC480Conversion.exe (Convert LightCycler 480 Raw Data Text File into Input Formar for LinRegPCR). The text file then is converted to a grid. All wells were selected and extracted. File was exported to excel.

Secondly, the excel file was analysed through LinRegPCR.exe program. The excel was imported into the program (DNA-binding dye and LightCyler 480 – converted raw data). Select all wells to be analysed. Then, press bottom to determine baselines. File was saved on excel as compact + complete.

3.13. %P and granular-PolyP of P deplete *C. reinhardtii* strains

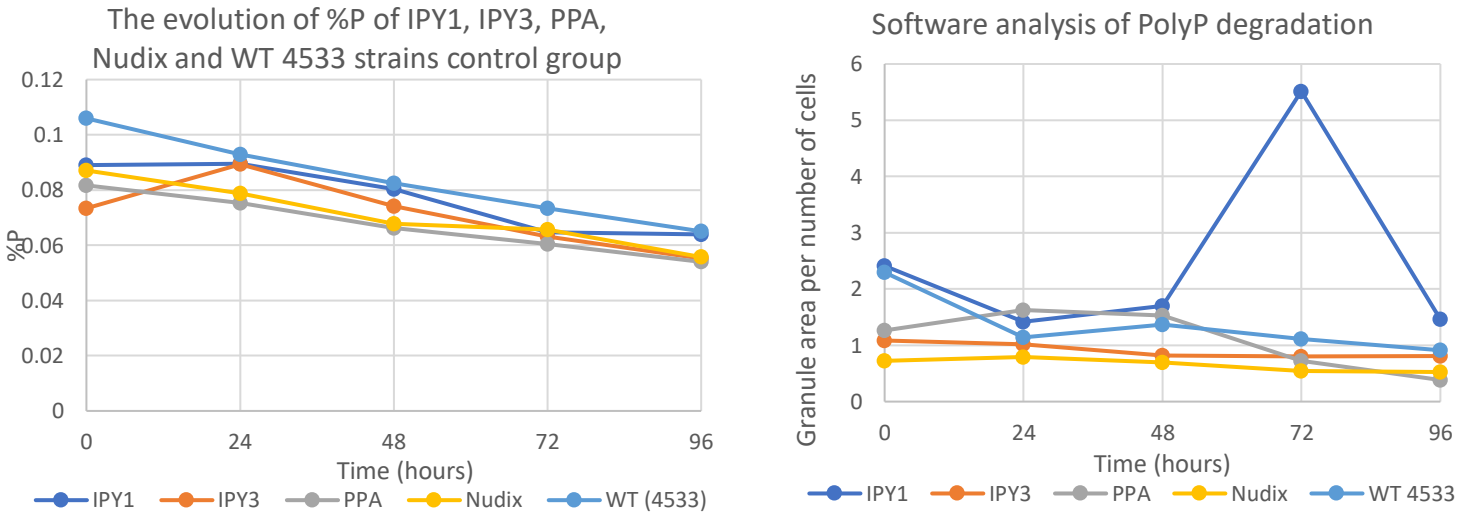

Figure 17: Analysis of the evolution of cellular P content of the IPY1, IPY3, PPA, Nudix and wild-type 4533 strains. Left: On the left, the evolution of the %P throughout the experiment before and after the addition of the P-shot (10 mg L^{-1} P). Right: The software analysis of the area occupied by PolyP granules per cell, before and after the addition of the P-shot.

3.14. Photographic comparison of different *C. reinhardtii* strains

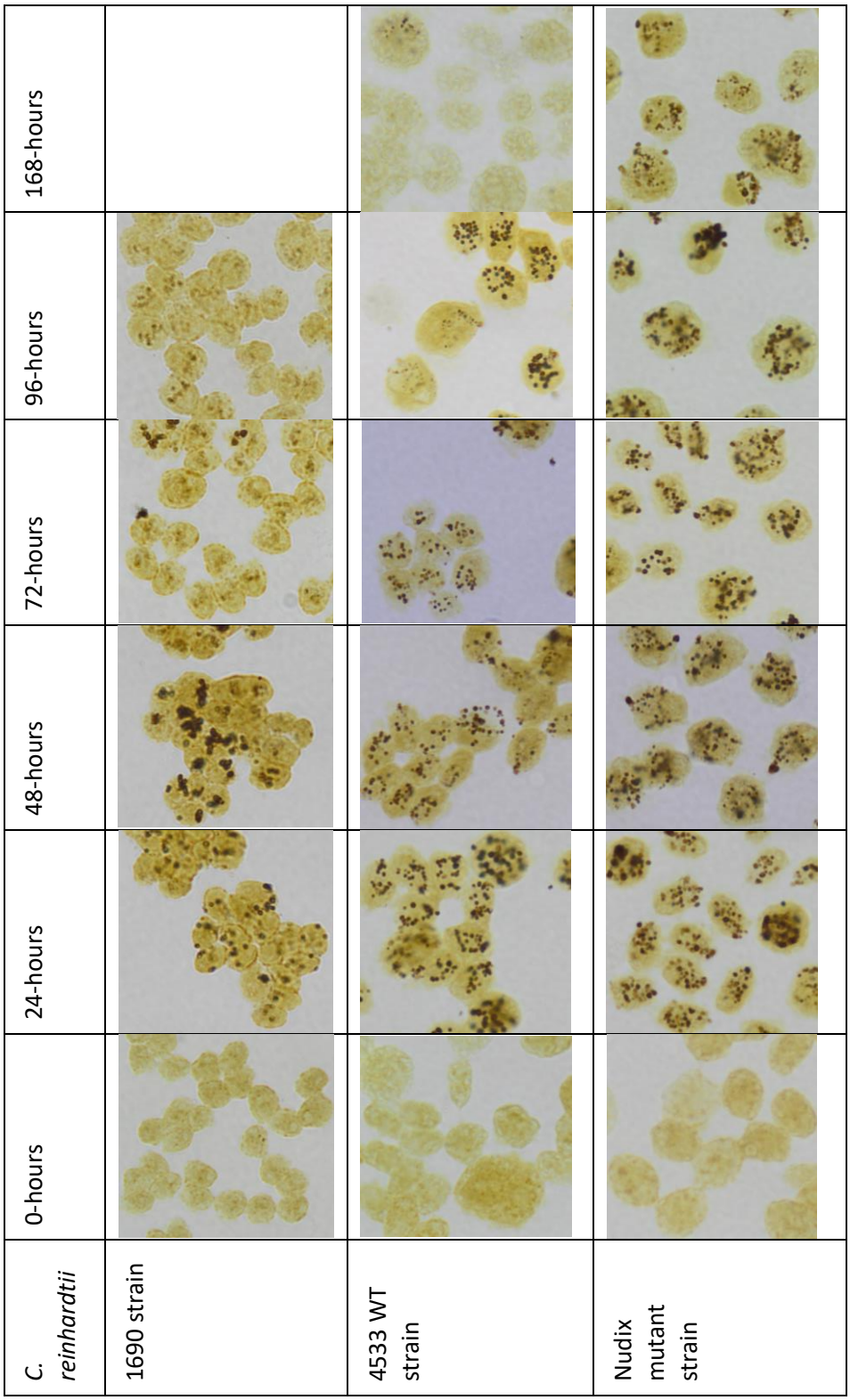

Figure 18: Comparison of PolyP degradation in *C. reinhardtii* 1690 wild-type, 4533 wild-type and Nudix mutant strains. The 0-hours samples were a representative of the control (no P) group.

3.15. Manual granule measurements

Number of granules	0	1	2	3	4	5	6+
	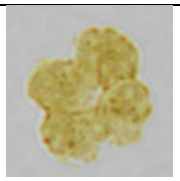	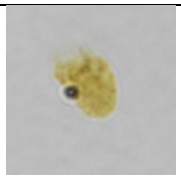		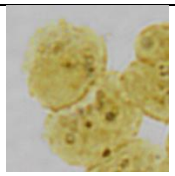	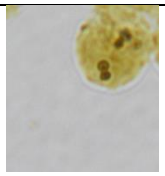	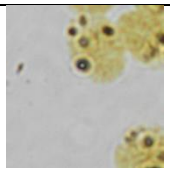	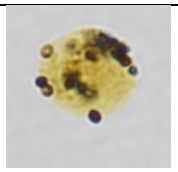
	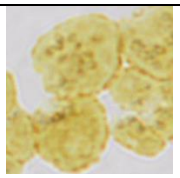	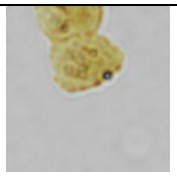	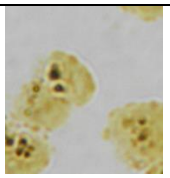	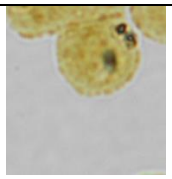	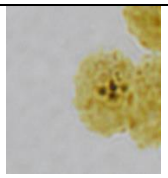	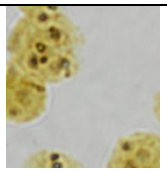	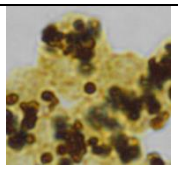

Figure 19: Examples of images used for establishing granule counts, showing cells containing the given number of granules (darkened regions).

3.16. Table of primers

Table 14: List of primers tested.

name	sequence	Tm
nudix 1F	CAACGCTATGGAGATTCAGG	60
nudix 1F2	CCTGTCAAGTTCTCGGGGTG	60
nudix 1R	CCTCCCAGCCGCCCTTAGG	59
nudix 2F	GCCAGTCAGCCGCCAC	60
nudix 2R	GAGCACCAGACGCGCT	59
nudix 3F	GGCCTCGTGTTTCCTAAGGG	60
nudix 3R	GATGTAGTATTTCCCGCTCGTGA	60
IPY1 1F	CGTGCGCTCGGTGACC	60
IPY1 1R	ACCCTGCTTGAAGAACAT	56
IPY1 2F	GGACGTGGAGAAGCACTT	56
IPY1 2R	TGCACTTGTTGTCGTAGC	55
IPY3 1F	GAAGAACGAGCACAAGGAGG	58
IPY3 1R	GGTACATGTTCAGCGAGTCC	55
IPY3 2F	AAAGATGTCCTTCTACAGGGGA	58
IPY3 2R	GTCCAGCTCATACTTGACCTTG	58
PPA 1F	AAGATGCTGGTGGTCAATGTC	58
PPA 1R	GGCAATCTTGTAGGTACGGAAGAA	60
PPA 2F	CAGTGGCAAGAGTCAAGAGC	58
PPA 2R	ACGTCTGGGTCTCAATCTTG	57
PPA 3F	ACGTCACTGCCATACAACCC	60
PPA 3R	CACGTCTGGGGGATGCCG	63
PPA 4F	CCTAGAGGTGGGCGGCG	62
PPA 4R	CATTGACCACCAGCATCTTCCAG	62
VTC1 1F	TAAGTCATATTTCGCCAACGAG	53
VTC1 1R	TGAACAGAGCGTAGCCCATGAT	58
VTC4 1F	GTCAACATCAACTACCTGGGCT	60
VTC4 1R	GTCCGAGTAGTTGCCCTGC	60
VTC4 1R2	TACAGGTTGGACAGCGACAC	60
VTC4 3F	TTCCAGATCCCCTTTGACGC	60
VTC4 3R	GGAAGCGCGTGATCTCGG	61
VTC4 3R2	GAGTCACCGGCAGCGAG	60
CBLP 2F	AAGATGGTCAAGGTCTGGAACCT	58
CBLP 2R	GTACAGGCGCTTGCCCTCAGCC	65